Viral and cellular mRNA-specific activators harness PABP and eIF4G to promote translation initiation downstream of cap binding

Richard W. P. Smith[a,b,c,1], Ross C. Anderson[a,b,2], Osmany Larralde[c,3], Joel W. S. Smith[b], Barbara Gorgoni[a,b,4], William A. Richardson[a,b], Poonam Malik[c,d,5], Sheila V. Graham[c], and Nicola K. Gray[a,b,1]

[a]Medical Research Council Centre for Reproductive Health, Queen's Medical Research Institute, University of Edinburgh, Edinburgh EH16 4TJ, United Kingdom; [b]Medical Research Council Human Genetics Unit, University of Edinburgh, Western General Hospital, Edinburgh EH4 2XU, United Kingdom; [c]Medical Research Council-University of Glasgow Centre for Virus Research, Garscube Campus, Glasgow G61 1QH, United Kingdom; and [d]Wellcome Trust Centre for Cell Biology and Institute of Cell Biology, University of Edinburgh, Edinburgh EH9 3BF, United Kingdom

Edited by Nahum Sonenberg, McGill University, Montreal, QC, Canada, and approved April 28, 2017 (received for review July 4, 2016)

Regulation of mRNA translation is a major control point for gene expression and is critical for life. Of central importance is the complex between cap-bound eukaryotic initiation factor 4E (eIF4E), eIF4G, and poly(A) tail-binding protein (PABP) that circularizes mRNAs, promoting translation and stability. This complex is often targeted to regulate overall translation rates, and also by mRNA-specific translational repressors. However, the mechanisms of mRNA-specific translational activation by RNA-binding proteins remain poorly understood. Here, we address this deficit, focusing on a herpes simplex virus-1 protein, ICP27. We reveal a direct interaction with PABP that is sufficient to promote PABP recruitment and necessary for ICP27-mediated activation. PABP binds several translation factors but is primarily considered to activate translation initiation as part of the PABP–eIF4G–eIF4E complex that stimulates the initial cap-binding step. Importantly, we find that ICP27-PABP forms a complex with, and requires the activity of, eIF4G. Surprisingly, ICP27–PABP–eIF4G complexes act independently of the effects of PABP-eIF4G on cap binding to promote small ribosomal subunit recruitment. Moreover, we find that a cellular mRNA-specific regulator, Deleted in Azoospermia-like (Dazl), also employs the PABP–eIF4G interaction in a similar manner. We propose a mechanism whereby diverse RNA-binding proteins directly recruit PABP, in a non–poly(A) tail-dependent manner, to stimulate the small subunit recruitment step. This strategy may be particularly relevant to biological conditions associated with hypoadenylated mRNAs (e.g., germ cells/neurons) and/or limiting cytoplasmic PABP (e.g., viral infection, cell stress). This mechanism adds significant insight into our knowledge of mRNA-specific translational activation and the function of the PABP–eIF4G complex in translation initiation.

DAZL | ICP27 | mRNA-specific translational regulation | mRNA-binding protein | poly(A)-binding protein

Despite the importance of translational control, the mechanisms by which specific subsets of mRNAs are translationally regulated are only well defined in a handful of cases. Nevertheless, it is clear that regulation is most often mediated by factors recruited to the 3′ untranslated region (UTR) of mRNAs and frequently occurs at the level of initiation (1). Initiation is a multistep process involving several mRNA-dependent steps, each of which requires eukaryotic initiation factors (eIFs) (2). Initially, the m^7GpppX cap is bound by eIF4F, comprising a large scaffold protein, eIF4G, bound to the cap-binding protein, eIF4E, and an RNA helicase, eIF4A. The small (40S) ribosomal subunit, initiator tRNA, and associated initiation factors are then recruited as a 43S preinitiation complex. Recruitment is facilitated by eIF4A-dependent removal of RNA secondary structure and by the interaction of 40S-associated eIF3 with eIF4G. The 43S small ribosomal subunit complex then scans the 5′ UTR to locate a start codon, recognition of which promotes release of initiation factors and joining of the large (60S) ribosomal subunit to form an 80S ribosome. Like the cap, the poly (A) tail serves as a primary determinant of translational efficiency (3) via the action of poly(A)-binding protein (PABP). Analysis of mRNA-ribosomal subunit association has shown that PABP promotes small subunit recruitment, an activity attributed to its ability to stimulate cap binding by eIF4E (4). Stabilization of the cap–eIF4E interaction requires the RNA-binding activity of their common partner, eIF4G (5), which acts as a bridging factor mediating the "closed-loop" mRNA conformation (1). This conformation brings the ends of the mRNA into proximity, providing insight into how 3′ UTR-bound factors can control initiation.

Despite the rate-limiting, cap-binding step being a common regulatory target for global and mRNA-specific regulation, studies of diverse mRNA-specific translational repressors have revealed that multiple initiation steps can be regulated (1). In contrast, mechanisms are described for only a very few

Significance

The majority of genes are controlled at the level of mRNA translation, with accurate regulation being critical to cellular function and health. The repression or activation of subsets of mRNAs, so-called "mRNA-specific" regulation, is often mediated by RNA-binding proteins. However, the mechanisms underlying mRNA-specific activation have only been determined in a very few cases. Here, we uncover a mechanism of mRNA-specific activation used by viral and cellular proteins, which share no sequence similarity, suggesting that it may represent a widespread mechanism. Importantly, in so doing, we also expand our knowledge of how two key translation factors, poly(A)-binding protein (PABP) and eukaryotic initiation factor 4G (eIF4G), function during translation initiation, showing they have pleiotropic effects on small ribosomal subunit recruitment.

Author contributions: R.W.P.S., O.L., and N.K.G. designed research; R.W.P.S., R.C.A., O.L., J.W.S.S., B.G., W.A.R., and N.K.G. performed research; R.W.P.S., R.C.A., O.L., P.M., S.V.G., and N.K.G. analyzed data; and R.W.P.S. and N.K.G. wrote the paper.

The authors declare no conflict of interest.

This article is a PNAS Direct Submission.

Freely available online through the PNAS open access option.

[1]To whom correspondence may be addressed. Email: nicola.gray@ed.ac.uk or r.smith@ed.ac.uk.

[2]Present address: Department of Immunology, Faculty of Health Sciences, University of Pretoria, Pretoria 0001, South Africa.

[3]Present address: Scottish National Blood Transfusion Service, Edinburgh EH17 7QT, United Kingdom.

[4]Present address: Public Engagement with Research Unit, University of Aberdeen, Aberdeen AB24 3FX, United Kingdom.

[5]Present address: STEM Laboratories & Research Office and Graduate School, University of Cumbria, Carlisle CA1 2HH, United Kingdom.

This article contains supporting information online at www.pnas.org/lookup/suppl/doi:10.1073/pnas.1610417114/-/DCSupplemental.

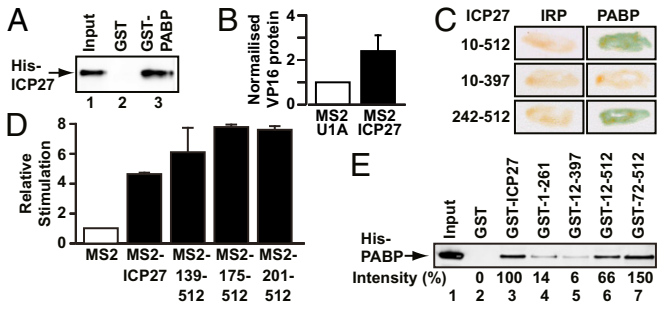

Fig. 1. PABP interacts directly with ICP27 regions required for translational stimulation. (*A*) Immobilized purified GST-PABP or GST was incubated with purified His-ICP27. ICP27 was detected by immunoblotting; input is 10%. (*B*) Oocytes expressing ICP27 or U1A (negative control) were injected with VP16 mRNA and luciferase mRNA as an internal control. VP16 protein levels normalized to luciferase activity are plotted (±SEM; $n = 5$). (*C*) Y2H analysis of PABP interactions with indicated ICP27 regions. Iron regulatory protein (IRP) was used as a negative control. (*D*) Oocytes expressing MS2, MS2-ICP27, or MS2-ICP27 truncations (Fig. S3*A*) were coinjected with m^7G-Luc-MS2$_3$ and β-gal mRNAs (Fig. S2*A*, [1] and [7]). Effects on translation were measured by luciferase assay normalized to β-gal activity. Translational stimulation relative to MS2 protein alone (=1) is plotted (±SEM; $n = 3$). (*E*) Immobilized purified GST or GST fusions of ICP27 or indicated truncations (Fig. S3*A* and Table S2) were incubated with purified His-PABP. PABP was detected by quantitative immunoblotting, and band intensities are shown, with the band intensity of lane 3 set to 100%. Input is 150%.

mRNA-specific translational activators, with these activators acting at the cap-binding step. Because studies of viruses have proved highly informative for the understanding of cellular translational regulation, we examined the mechanism of action of ICP27, an essential herpes simplex virus type 1 (HSV-1) protein that is a key regulator of host and viral gene expression (6). ICP27 regulates the translation of a subset of viral mRNAs, including the viral mRNAs encoding VP16 and ICP5 (7, 8), via an uncharacterized mechanism. This effect is mRNA-specific, because the translation of other studied viral and cellular mRNAs is not ICP27-dependent (7, 8). We posited that elucidating this mechanism may provide insight into cellular mRNA-specific regulators because HSV-1 mRNAs are, like most cellular mRNAs, capped, polyadenylated, and translated via the canonical cap-dependent pathway described above. HSV-1 infection is accompanied by posttranslational modification of some initiation factors (9) and by relocalization of PABP to the nucleus (10, 11); however, similar modifications of the translational machinery occur in noninfected cells, for example, as a result of cellular stress (12, 13).

Consistent with its role as an mRNA-specific translational activator (7, 8, 14), ICP27 binds RNA, cosediments with polyribosomes (14), and can be isolated with components of the translational machinery (10, 15). Because ICP27 can stimulate translation in the absence of other viral proteins when tethered to the 3′ UTR of reporter mRNAs (14), its interaction with the translational machinery must either be direct or mediated indirectly by other cellular proteins, further supporting the idea that it may share a mechanism of action with cellular regulators of translation. Here, we investigate its mechanism of action, establishing that it requires recruitment of PABP, via a direct protein interaction, to ICP27-bound mRNAs. ICP27 activity was also shown to depend on the integrity of eIF4G, but was surprisingly found to stimulate small subunit recruitment downstream of the initial cap-binding event. Furthermore, we provide evidence that this previously undescribed mechanism of mRNA-specific translational activation also applies to at least one cellular mRNA-binding protein, Deleted in Azoospermia-like (Dazl). These results increase our knowledge of the mechanisms of mRNA-specific translational activation and provide evidence that the PABP–eIF4G interaction in metazoans has pleiotropic effects on small ribosomal subunit recruitment.

Results

PABP Interacts with the Region of ICP27 That Stimulates Translation. Previous studies found that ICP27 can be isolated in RNase-sensitive complexes with multiple initiation factors (10, 15) and can interact directly with eIF3 subunits in pull-down experiments (15), raising the possibility that it may function by interacting with one or more initiation factors. This possibility prompted us to screen for such interactions by directed yeast two-hybrid (Y2H) analysis, revealing a single strong interaction with PABP (Table S1). In keeping with this finding, PABP was coimmunoprecipitated with ICP27 from HSV-1–infected cell extracts (Fig. S1 *A* and *B*), with RNase treatment reducing coimmunoprecipitation efficiency (Figs. S1 *A*, lanes 3–6 and *B*, lanes 3–4), presumably by eliminating mRNA-mediated coisolation (Fig. S1*C*). To examine whether this association may be functionally relevant, we initially tested whether it is direct. Pull-down experiments with purified recombinant proteins (Fig. S1 *D* and *E*) in the presence of RNase showed that GST-PABP, but not GST alone, binds His-ICP27 (Fig. 1*A*). In the reciprocal experiment, purified GST-ICP27 and His-PABP (Fig. S1 *F* and *G*) also interact (Fig. S1*H*). These results establish a direct protein–protein interaction in the absence of bridging eukaryotic proteins or RNA (see also Figs. 1 *C* and *E* and 2 *A* and *B*).

To determine whether its interaction with PABP underlies the ability of ICP27 to stimulate translation, ICP27 regions associated with this activity and their interaction with PABP were probed. Tether-function analysis (Fig. S2*A*) is ideally suited for delineating functional protein regions because it permits the separation of RNA-binding and activation domains (16). Importantly, we previously established that tethering ICP27 to the 3′ UTR of reporter mRNAs recapitulates the robust mRNA-specific effect on translation of target mRNAs observed in infected cells (7, 14), with only reporters to which ICP27 is tethered being translationally activated (14). In contrast, translational stimulation of target mRNAs (e.g., VP16) by untethered ICP27 is inefficient outside of the context of

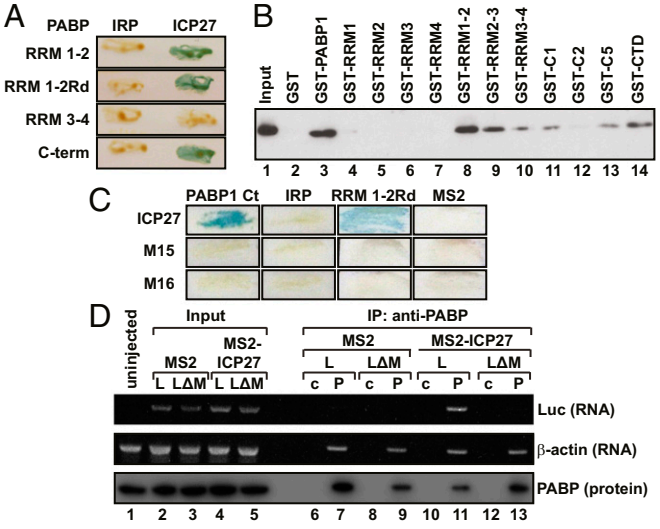

Fig. 2. Translationally active ICP27 interacts with two domains of PABP and recruits PABP to mRNA. (*A*) Y2H analysis of ICP27 interactions with PABP domains. IRP was used as a negative control. (*B*) Immobilized purified GST or GST fusions of PABP or indicated truncations (Table S2) were incubated with HSV-1–infected cell extracts in the presence of RNase 1. ICP27 was detected by immunoblotting. (*C*) Y2H analysis of the PABP C-terminus (Ct, amino acids 396–633), RRM1-2Rd with ICP27 (amino acids 10–512), or ICP27 containing the M15 or M16 mutation. IRP and MS2 were used as negative controls. (*D*) Oocytes expressing MS2 or MS2-ICP27 were injected with ApG-Luc-MS2$_3$ (L) or ApG-Luc-ΔMS2 (LΔ) (Fig. S2*A*, [2] and [6]). PABP was immunoprecipitated (P) from lysates [control: nonspecific rabbit IgG (c)] and detected by immunoblotting (input is 27%). The presence of copurified luciferase or endogenous β-actin mRNAs was assessed by RT-PCR.

infection (Fig. 1*B* and Fig. S2 *B* and *C*), suggesting that an unidentified ancillary viral factor, which can be substituted by tethering, may normally aid its RNA-binding specificity. Tethering studies were performed in *Xenopus laevis* oocytes, which offer a unique opportunity to analyze multifunctional regulators (16) because reporter mRNAs can be directly microinjected into the cytoplasm, permitting effects on translation to be studied independent of ICP27 roles in regulating mRNA transcription, processing, and nuclear export (17). Furthermore, mRNAs remain remarkably stable in oocytes even without a functional cap or poly(A) tail (Fig. S2*D*) (18), providing an opportunity for detailed mechanistic analysis in intact cells. Previous analysis also revealed that the C-terminal 105 amino acids of ICP27 are essential to stimulate translation (14), suggesting that factors required for this activity interact with this region. Importantly, in this regard, Y2H analysis shows that the PABP-binding site lies within the C-terminal 115 amino acids (Fig. 1*C*, compare amino acids 10–512 and amino acids 10–397 and Fig. S3*A*). By contrast, we find that the N-terminal region is dispensable both for translational stimulation (Fig. 1*D*, MS2-139–152, MS2-175–512, and MS2-201–512 and Fig. S3*A*) and PABP binding (Fig. 1*C*, amino acids 242–512). Because the N-terminal region contains the RNA-binding domain (RGG-box), this result lends weight to the RNA independence of the ICP27–PABP interaction. Similar results were obtained by GST pull-down of purified PABP with ICP27 domains in the presence of RNase 1 (Fig. 1*E*, Fig. S3*B*, and Table S2). Taken together, these results show that PABP interacts with the region of ICP27 responsible for its ability to promote translation.

Translationally Inactive Mutants of ICP27 Fail to Interact with PABP. PABP1 comprises several functional domains known to mediate RNA and/or protein interactions (19) (Fig. S3*C*). Y2H analysis revealed that ICP27 interacts strongly with the RNA-recognition motifs (RRMs) 1–2 (residues 3–182) as well as with the C-terminal region (residues 395–633) of PABP1 (Fig. 2*A*). Dual binding sites have been described for several other PABP partner proteins (20). Because both ICP27 and PABP are RNA-binding proteins, RRM1-2Rd (Y56V, F142V) (16), an RNA-binding–deficient mutant of RRM1-2, was used to confirm further that their interaction is not RNA-mediated (Fig. 2*A*). The C terminus of PABP does not bind RNA (19). To verify these results, PABP1 domains were purified as GST fusions (Fig. S3*D* and Table S2) and used in pull-down assays in the presence of RNase 1. Fig. 2*B* shows that although no single RRM (lanes 4–7) interacts with ICP27, RRM1-2 (lane 8) and the C-terminal region (lane 14) interact, confirming our Y2H mapping. RRM2-3 (lane 9) also shows significant interaction with ICP27, whereas RRM3-4 (lane 10) interacts only weakly, indicating that ICP27 has strong affinity for a region within the N-terminal 190 amino acids of PABP1. The PABP1 C-terminal domain is composed of a proline-rich linker and the PABC domain (Fig. S3*C*), and further mapping showed that ICP27 interacts with the N-terminal portion of the linker region (present in C1 and C5 but not in C2; Fig. 2*B*, lanes 11–14). Interestingly, several C-terminal amino acid substitutions [M15 (P465L, G466E) or M16 (C488L)] (21) abrogate the ability of ICP27 to associate with polyribosomes in infected cells and to stimulate translation when tethered (14), providing a tool with which to probe further the importance of PABP binding. Following delineation of the ICP27-binding sites in PABP, the interaction of the translationally inactive ICP27 mutants (M15 and M16) with these binding sites was examined by Y2H analysis and immunoprecipitation from cells infected with M15/M16 mutant virus. Critically, both point mutants failed to interact with PABP1 (Fig. 2*C* and Fig. S3*E*), directly linking ICP27 activity and PABP binding, leading us to conclude that this interaction is crucial for ICP27-mediated translational stimulation.

ICP27 Recruits PABP to mRNA. The dependence of ICP27 activity on PABP binding raised the hypothesis that ICP27 may function to promote PABP recruitment to specific mRNAs. To test this hypothesis, RNA coimmunoprecipitations of tethered unadenylated reporter mRNAs were performed using antibodies against PABP (Fig. 2*D*). Critically, PABP fails to associate with these mRNAs unless they contain MS2-binding sites (Fig. 2*D*, lanes 11 and 13) and unless MS2-ICP27, rather than MS2 alone (lanes 7 and 11), is present. Endogenous polyadenylated β-actin mRNA, which binds PABP directly via its poly(A) tail, was a positive control. Thus, MS2-ICP27 is sufficient to bridge the association of PABP with the reporter mRNA, providing strong direct support for a mechanism by which ICP27 functions to enhance the recruitment of PABP to mRNA. In keeping with this finding, manipulating poly (A) tail status, and thus poly(A)-mediated recruitment of PABP to the reporter mRNAs, alters the relative magnitude of stimulation by tethered ICP27 (Fig. S4 *A* and *B*).

ICP27 Stimulates Initiation of Translation Independently of the Cap-Binding Event. In metazoan cells, PABP drives small ribosomal subunit recruitment, a function attributed to enhancement of cap binding by eIF4E, as part of the PABP–eIF4G–eIF4E complex (2, 4). Therefore, our results raise the possibility that ICP27, like other mechanistically defined mRNA-specific activators, may exert its effect at the initial cap-binding step (22, 23). To address this possibility, the ability of MS2-ICP27 to stimulate a reporter mRNA bearing a nonfunctional ApppG-cap structure (Fig. S2*A*, [2]) was tested. ApppG-capped mRNAs are stable (Fig. S2*D*), although translated at low efficiency (Fig. S5*A*), because they are not recognized by eIF4E. Surprisingly, ICP27 activates the translation of this reporter mRNA to a similar extent as the m^7GpppG-capped reporter (Fig. S5*B*). Thus, the 5′ cap-recognition event appears dispensable for translational activation by tethered ICP27, suggesting that it activates via an undescribed mechanism. Because the inherent instability of purified ICP27 confounds cell-free system analysis of initiation intermediates (e.g., by sucrose gradients), we used reporters with different viral internal ribosome entry sites (IRESs) to further delineate its mechanism of action in intact cells. Critically, these IRESs have distinct, well defined, noncanonical mechanisms to recruit small ribosomal subunits and are functional in *X. laevis* oocytes (24) (Fig. S5*A*). Hepatitis A virus (HAV) RNA, like many other IRES-driven viral RNAs, lacks a physiological cap and does not require the cap–eIF4E interaction for its translation, although it may use eIF4E noncanonically (25, 26). Importantly, HAV IRES-mediated initiation is stimulated by ICP27 (Fig. 3*A* and Fig. S2*D*), verifying that cap recognition is not required for MS2-ICP27 action. The eIF4E independence of ICP27 was probed further using a poliovirus (PV) IRES-dependent reporter mRNA because eIF4E is dispensable for PV translation (27). PV-IRES translation is stimulated to levels comparable to the m^7GpppG-capped reporter (Fig. 3*B* and Fig. S2*D*), establishing that neither the cap nor the cap-binding protein is required for ICP27-mediated activation. These findings suggest that the ICP27–PABP complex acts downstream of cap binding to stimulate ribosomal subunit recruitment. To test this possibility, a reporter mRNA containing the classical swine fever virus (CSFV) IRES was used. Small subunit recruitment by the CSFV IRES differs significantly from both canonical initiation (28) and small subunit recruitment at HAV and PV IRESs (25) in that it is independent of all eIF4 factors and eIF3 (28, 29). Crucially, the ability of ICP27 to stimulate translation was completely abrogated on CSFV IRES-driven reporter mRNAs (Fig. 3*C* and Fig. S2*D*). This result contrasts with the ability of some translational repressors that target 60S joining to regulate translation of such mRNAs (30). Thus, taken together, these results establish that the ICP27–PABP complex acts during initiation but downstream of cap binding to enhance small subunit recruitment through one or more of the initiation factors required by PV but not CFSV (i.e., eIF4G, eIF4A, eIF4B, eIF3). Because this finding was unexpected, we directly tethered PABP, recapitulating the reporter mRNA translational stimulation by ICP27 (Fig. S5*C*), consistent with PABP mediating the effects of ICP27 and being able to activate small subunit recruitment independently of its ascribed effects on cap binding.

Downstream Effectors of the ICP27–PABP Interaction. Because ICP27, surprisingly, does not enhance small subunit recruitment via a PABP-eIF4G-eIF4E–mediated effect on cap binding, we

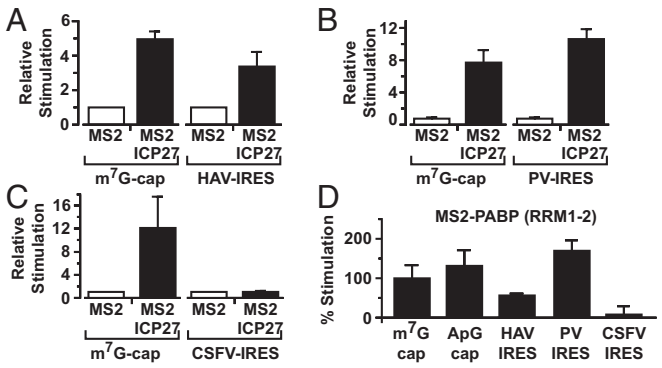

Fig. 3. Tethered ICP27 stimulates small ribosomal subunit joining independently of cap binding. Oocytes expressing MS2 or MS2-ICP27 were coinjected with β-gal mRNA and m^7G-Luc-MS2$_3$ or HAV-Luc-MS2$_3$ mRNA (*A*), PV-Luc-MS2$_3$ mRNA (*B*), or CSFV-Luc-MS2$_3$ mRNA (*C*) (Fig. S2*A*). Data ($n = 3$) are plotted as in Fig. 1*D*. (*D*) Oocytes expressing MS2 or MS2-PABP (RRM1-2) were coinjected with the reporter and control mRNAs as above. The plot represents luciferase activity (corrected for β-gal activity) of each reporter with MS2–RRM1-2 divided by the luciferase activity with MS2 alone. The m^7G-Luc-MS2$_3$ ratio is set to 100%.

investigated which PABP partner(s) transduce(s) its effects. PABP interacts with several initiation factors through different domains (Fig. S3*C*); thus, we tested which of these domains is sufficient to recapitulate the effect of ICP27 when directly tethered to our reporter mRNA panel. Interestingly, RRM1-2 (Fig. 3*D*) efficiently stimulated the translation of m^7GpppG-capped (set to 100%), ApppG-capped, and HAV-IRES and PV-IRES reporters, but not the translation of a CSFV IRES reporter, reproducing the effects of MS2-ICP27 and MS2-PABP. This result indicates that eIF4G and/or Paip1, a translation factor with homology to eIF4G, both of which bind RRM1-2 (Fig. S3*C*), may serve as a downstream effector of ICP27 activity.

PABP Forms a Complex with ICP27 and eIF4G. Because we have shown that ICP27 does not interact directly with eIF4G or Paip1 (Table S1) (15), a role for these factors would require that ICP27 and eIF4G or Paip1 interacts with PABP simultaneously. Because an interaction of ICP27 with RRM1-2 could disrupt eIF4G or Paip1 binding, we tested whether their binding sites are separable. Fig. 4*A* shows that ICP27 binds a region of RRM1-2 that binds Paip1 but not eIF4G (RRM1-2Nt) (16) suggesting that ICP27 and eIF4G may be able to interact simultaneously with PABP. To probe directly whether PABP can bridge ICP27 and eIF4G, GST pull-downs with purified recombinant proteins (Figs. S1 *F* and *G* and S6*A*) were performed. These pull-downs confirmed that eIF4G and ICP27 do not detectably interact directly and revealed that eIF4G associates with GST-ICP27 only in the presence of PABP, consistent with the formation of an ICP27–PABP–eIF4G complex (Fig. 4*B*).

Stimulation of Translation by ICP27-PABP Requires eIF4G. Cap binding is enhanced by eIF4G, but eIF4G also has a direct role in small subunit recruitment. Thus, to ascertain whether it is functionally targeted in ICP27-mediated translational activation, modified tether-function assays were undertaken in which mRNAs encoding picornavirus 2A protease (2Apro) or U1A (negative control) were coinjected with reporter mRNAs. Cleavage by 2Apro separates an N-terminal part of eIF4G that binds eIF4E and PABP from the C-terminal part that binds RNA, eIF4A, and 40S subunit-associated eIF3 (20). A *lacZ* mRNA containing the eIF4G-independent, 2Apro-insensitive CSFV IRES served as a critical internal control (Figs. S2*A*, [8] and S6*B*). *X. laevis* eIF4G, but not Paip1 or PABP, is efficiently cleaved by 2Apro (Fig. S6*C*), allowing us to test specifically the requirement for eIF4G in ICP27-mediated translational stimulation. ICP27 contains no predicted 2Apro cleavage sites (www.cbs.dtu.dk/services/NetPicoRNA/). Critically, stimulation by tethered PABP and ICP27 is reproducibly decreased in the presence of 2Apro (Fig. 4*C*). By contrast, 2Apro does not alter translational stimulation by tethered stem-loop–binding protein (SLBP) (Fig. 4*C*), a translational activator that acts independently of the PABP–eIF4G interaction (23, 24). This result establishes eIF4G as the PABP partner required to mediate the cap-independent effects of ICP27 on translation initiation. Thus, our results support a model for mRNA-specific activation in which formation of an alternative closed-loop complex comprising a 3′ UTR-bound mRNA-specific activator, PABP, and eIF4G stimulates the small ribosomal subunit recruitment step directly, downstream of the ascribed effects of the PABP–eIF4G complex in promoting cap binding (Fig. 5*A*, step 2).

A Cellular Activator Shares this Mechanism. Our results raise the possibility that other viral or cellular proteins might use this PABP-dependent, cap-independent mechanism. Of particular interest were observations pertaining to Dazl, a 3′ UTR-bound regulator essential for germ cells. Germ cells often store mRNAs with short poly(A) tails; Dazl can stimulate the initiation of nonadenylated mRNAs at an undefined step but requires PABP interaction for this activity (31). Because these shared properties suggest it may use the mechanism defined for ICP27, we compared its mode of action with the mode of action of ICP27. Importantly, we find that Dazl-mediated activation is also 2A-protease–sensitive (Fig. 5*B*) [Dazl contains no predicted 2Apro cleavage sites (www.cbs.dtu.dk/services/NetPicoRNA/)] and that Dazl recapitulates the pattern of stimulation of the panel of reporter mRNAs observed with ICP27 (Fig. 5 *C* and *D* and Fig. S6*D*), revealing that this PABP-interacting translational activator shares with ICP27 the ability to activate translation in an eIF4G-dependent manner downstream of cap binding. These results strongly imply that the elucidated ICP27 mechanism is relevant to regulation of translation by cellular RNA-binding proteins.

Discussion

By exploring the function of ICP27, we have uncovered a mechanism for mRNA-specific activation that cannot be explained in terms of existing models that describe enhancement of the rate-limiting

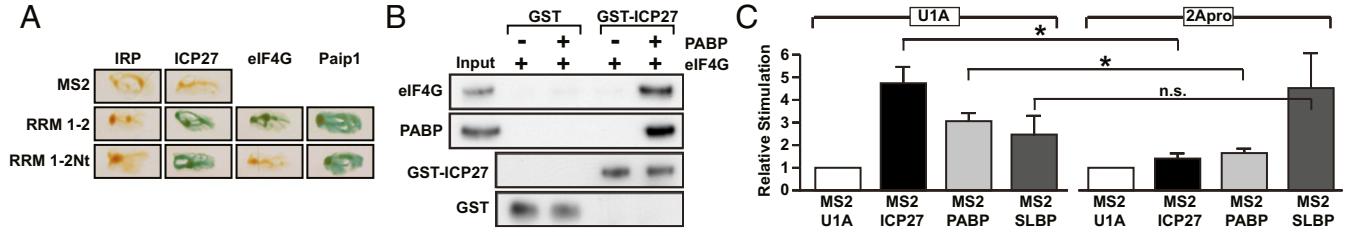

Fig. 4. ICP27-PABP–mediated translational stimulation is dependent on eIF4G. (*A*) Y2H of PABP RRM1-2 (amino acids 1–182) or RRM1-2Nt (amino acids 3–137) with ICP27 (amino acids 10–512), eIF4G (amino acids 1–641), or Paip1. MS2 and IRP were used negative controls. (*B*) Immobilized purified GST-ICP27 or GST was incubated with purified FLAG-eIF4G and/or His-PABP as indicated. Proteins were detected by immunoblotting. (*C*) Oocytes expressing MS2-U1A (negative control), MS2-ICP27, MS2-PABP, or MS2-SLBP were injected with m^7G-Luc-MS2$_3$ and CSFV–β-gal mRNAs as well as mRNAs expressing either 2Apro or U1A ($n = 4$; ±SEM). *$P < 0.05$; not significant (n.s.), $P > 0.05$.

CELL BIOLOGY

cap-binding event. Rather, we find that ICP27 and Dazl recruit PABP, which can exert an effect downstream of this initial cap-binding event, and is therefore not dependent on eIF4E (Fig. 5*A*, step 1) but nonetheless uses the PABP-partner protein eIF4G to promote small subunit recruitment. This analysis informs both on mechanisms of mRNA-specific translational activation and, more broadly, on the function of the PABP–eIF4G complex in initiation. Our data confirm reports that PABP coimmunoprecipitates with ICP27 (10, 15) (Fig. S1) and extend those reports by showing that the RNase-insensitive fraction reflects a direct ICP27–PABP interaction (Fig. 1 and Fig. S1), because both RNase-treated purified proteins and domains/mutants of PABP and ICP27 that do not bind RNA interact. In contrast, ICP27 fails to interact detectably with other tested translation factors (Table S1). We demonstrate the function of this interaction: ICP27 recruits PABP to mRNAs, and its abilities to bind PABP and to activate translation are linked (Fig. 2) (14), with the latter also requiring eIF4G (Fig. 4). ICP27-PABP-eIF4G–dependent activation of initiation (Figs. 3–5*A*) is consistent with the disassociation of VP16 mRNA from polysomes during infection with ICP27-deficient viruses (7); with coisolation of ICP27 with PABP, eIF4G, and eIF3 from infected cells (15); and with the dependence of translational activation of both natural target mRNAs (8) and tethered reporter mRNAs (14) on the PABP-interacting C terminus of ICP27 (8, 14) (Fig. 1), as well as with point mutations therein that abrogate PABP binding disrupting translation of reporter mRNAs and polysome association in infected cells (14). Our observations that the magnitude of ICP27-mediated stimulation is poly(A)-tail–sensitive (Fig. S4) and that tethered PABP can functionally substitute for ICP27 in stimulating mechanistically distinct reporter mRNAs (Fig. S5*C*) provide further support for the role of PABP. Our proposed model of translational stimulation by ICP27-PABP-eIF4G downstream of cap binding is supported by the following data: Tethering the eIF4G-binding domain of PABP to reporter mRNAs with different mechanisms of small subunit joining recapitulates the effects of ICP27 (Fig. 3), eIF4G can form a complex with ICP27 and PABP, and proteolytic cleavage of eIF4G abrogates translational stimulation (Fig. 4).

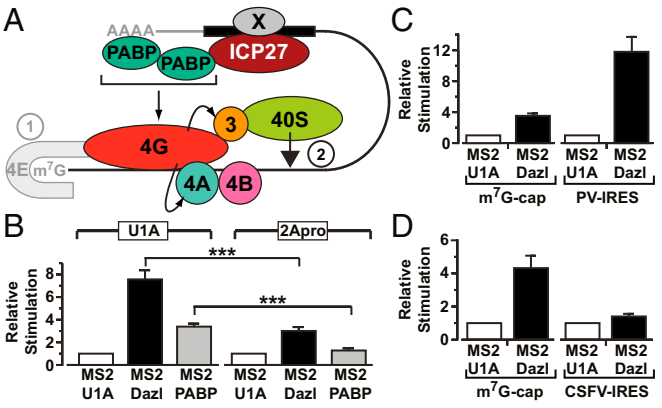

Fig. 5. (*A*) Model for ICP27-mediated translational stimulation of HSV-1 mRNA. ICP27 (red) binds to the translational target mRNA (solid black bar, putative ICP27-binding site) and recruits PABP (green). ICP27 target binding may be aided by an additional viral factor (Fig. 1*B*), denoted by X. Herpesvirus mRNAs have a 5′ cap (m^7G) and 3′ poly(A) tail; however, these structures and eIF4E (gray) are dispensable for ICP27-mediated translational activation. Rather, the ICP27–PABP complex promotes small ribosomal subunit recruitment through eIF4G, which interacts with eIF3 and eIF4A (curved arrows): eIF4A removes the secondary structure to allow small subunit binding, which is facilitated by direct eIF4G–eIF3 interactions. The eIFs are represented by their numbers. Steps of translation initiation: ①, cap binding; ②, 43S recruitment. (*B*) Oocytes expressing MS2-U1A (negative control), MS2-Dazl, or MS2-PABP were injected with m^7G-Luc-$MS2_3$ and CSFV-β-gal mRNAs as well as mRNAs expressing either 2Apro or U1A. ($n = 6$; ±SEM). ***$P < 0.001$. Oocytes expressing MS2-U1A or MS2-Dazl were coinjected with β-gal mRNA and m^7G-Luc-$MS2_3$ or with PV-Luc-$MS2_3$ mRNA (*C*) or CSFV-Luc-$MS2_3$ mRNA (*D*) ($n = 3$).

Previous analysis using PABP-depleted extracts to examine mRNA and ribosome subunit association established that PABP predominantly promotes small subunit recruitment, a function ascribed to its ability to promote eIF4E cap binding in a manner that is dependent on RNA binding by eIF4G (4, 5). However, our results firmly establish that the cap, eIF4E (Fig. 3), and the poly(A) tail (14) (Figs. 1, 3, and 5) are dispensable for ICP27/Dazl function, indicating that the effects on small subunit recruitment revealed by comparison of HAV/PV and CSFV IRESs (Fig. 3) are independent of enhanced cap or poly(A) binding. Rather, our results are most consistent with PABP-eIF4G effects on initiation not acting exclusively via cap binding by eIF4E, but more broadly to promote eIF4G function: enhancing its direct role in small subunit recruitment (Fig. 5*A*, step 2), namely, delivery of eIF4A, which creates an unstructured subunit-binding site, and its interaction with eIF3, which facilitates small subunit recruitment (2). This mechanism is consistent with the coisolation of ICP27 with PABP, eIF4G, and eIF3 (15) in infected cells and with the eIF4G, eIF4A, and eIF3 independence of CSFV IRES-driven 40S recruitment (28), in contrast to recruitment mediated by the HAV or PV IRESs (25, 27, 32). It is also consistent with the idea that PABP may enhance RNA binding by eIF4G (5), which would be expected to increase the efficiency of all eIF4G-dependent steps and not selectively those steps mediated via eIF4E. Thus, although our analysis has allowed the effects of the PABP–eIF4G complex on downstream events to be recognized, informing on both mRNA-specific activation and the role of the PABP–eIF4G complex during initiation, it does not exclude that ICP27/Dazl–PABP–eIF4G complexes can also enhance cap binding.

Our work highlights a way in which viruses target PABP function to hijack the host translational machinery (20). However, because HSV-1 mRNAs are capped and polyadenylated (9), the question is raised of why their translation should require an additional means of PABP recruitment. Although translation is not shut down during HSV-1 infection, it is partially impeded [in addition to widespread destruction of mRNAs (9)], necessitating the involvement of virus-encoded proteins to augment initiation efficiency, as exemplified by ICP6-mediated stimulation of otherwise suboptimal eIF4F assembly (6). Thus, ICP27 may function in this capacity by targeting small subunit recruitment via PABP-eIF4G to promote the translation of specific viral mRNAs, two of which (VP16 and ICP5) have been identified to date. Intriguingly, PABP is relocalized to the nucleus in an ICP27-independent manner at late times postinfection (10, 11), suggesting that ICP27 may provide a means to direct limiting amounts of cytoplasmic PABP to a subset of viral mRNAs late in infection (7, 8). Moreover, because PABP nuclear export is largely mRNA-driven in mammalian cells (12), and ICP27 promotes export of viral mRNAs (17), it is possible that the ICP27–PABP interaction may allow nuclear-retained PABP to be recruited and exported on these mRNAs, enabling their efficient translation. Specific binding of ICP27 to mRNAs that it translationally activates may be aided by another viral factor (Fig. 1*B*).

In being able to activate initiation downstream of cap binding, ICP27 differs from other mechanistically defined mRNA-specific translational activators. Serine arginine splicing factor 1 (SRSF1/SF2/ASF) promotes initiation by releasing eIF4E from 4E-BP sequestration, permitting eIF4E-eIF4G binding (22). SLBP and rotavirus nonstructural protein 3 (NSP3) bind unadenylated mRNAs, forming end-to-end complexes with eIF4E and eIF4G, but not with PABP (23, 33). In contrast to ICP27, SLBP fails to activate cap-independent translation (24) and NSP3-mediated activation is enhanced by the 5′ cap (33).

Our results reveal that the PABP–eIF4G interaction is a target not only for global and mRNA-specific repression (34) but also for mRNA-specific activation, highlighting the regulatory importance of this complex. Our analysis of Dazl, which activates the translation of hypoadenylated germ-cell mRNAs (31), shows that this PABP-eIF4G–dependent effect on 43S joining can be extended to at least one cellular mRNA-specific translational activator (Fig. 5). Because Dazl and ICP27 share no sequence homology, this finding indicates that different motifs can recruit PABP to mediate translational activation, suggesting that this mechanism may be used by a wide

variety of proteins. However, the function of PABP-recruiting proteins may also be affected by other partners, and recruited PABP would need to maintain its interactions with initiation factors to mediate activation. Interestingly, during the course of this study, a new cellular 3′ UTR-bound mRNA-specific activator, DAZAP1, was identified and found to be able to stimulate translation independently of the cap (35). Although a mechanism has not been determined for DAZAP1 function, its ability to stimulate translation does not appear to involve a direct interaction with eIF4G (35); thus, it is tempting to speculate that DAZAP1 may use PABP or another factor to mediate binding to eIF4G to promote events downstream of cap binding. This concept is reminiscent of the "variations on a theme" observed for 3′ UTR-bound repressors that directly (e.g., Bicoid) or indirectly (e.g., Bruno) contact eIF4E or its homologs to block association with eIF4G (1).

In summary, our results indicate that mRNA-specific activators can regulate small subunit joining through PABP–eIF4G interaction by a means other than via enhanced cap binding. Such a "cap- and poly (A) tail-independent" and PABP- and eIF4G-dependent mechanism would permit the translation of specific mRNAs under a variety of biological conditions: translational activation of hypoadenylated mRNAs (e.g., in germ cells or neurons), maintaining translation during viral infection or cell stress when PABP becomes predominantly nuclear, or conceivably when cap-dependent translation is repressed by 4E-binding proteins. Detailed analysis of other mRNA-specific regulators will reveal the extent to which this mechanism forms a paradigm for the action of other PABP-binding activators.

Materials and Methods

Plasmids, Cells, Viruses, and Antibodies. Detailed information on plasmids, cells, viruses, and antibodies is provided in *SI Materials and Methods*.

Tether-Function Assay. Tether-function assays were performed as described (16) except for experiments with 2A protease, as described in *SI Materials and Methods*.

Protein Expression and Purification. GST, GST-fusion proteins, His-ICP27, and His-PABP1 were expressed in *Escherichia coli* BL21 (DE3) pLysS (Novagen). Details of purifications are provided in *SI Materials and Methods*.

Protein Interaction Assays. Details of GST pull-downs, (RNA) coimmunoprecipitation, and Y2H assays are provided in *SI Materials and Methods*.

ACKNOWLEDGMENTS. We thank G. Belsham, J. Brosius, M. Hentze, A. Nieto, S. Morley, S. Rice, and N. Sonenberg for reagents and numerous colleagues for helpful discussions. Work in the N.K.G. laboratory was funded by Medical Research Council (MRC) Senior Fellowship G117/564, MRC Unit funding MC_U127692697 (to N.K.G.), and Wellcome Trust (084359/Z/07/Z) and Biotechnology and Biological Sciences Research Council (BB/I02137X/1) project grants (to N.K.G. and R.W.P.S.). Work in the S.V.G. laboratory was funded by MRC Program Grant G9826324. P.M. was a Royal Society Dorothy Hodgkin Fellow (RG090330). O.L. was funded by an MRC PhD studentship (G78/7826).

1. Hentze MW, Gebauer F, Preiss T (2007) *cis*-Acting regulatory sequences and trans-acting factors in translational control. *Translational Control in Biology and Medicine*, eds Mathews MB, Sonenberg N, Hershey JWB (Cold Spring Harbor Laboratory Press, Cold Spring Harbor, NY), pp 269–295.
2. Jackson RJ, Hellen CU, Pestova TV (2010) The mechanism of eukaryotic translation initiation and principles of its regulation. *Nat Rev Mol Cell Biol* 11:113–127.
3. Michel YM, Poncet D, Piron M, Kean KM, Borman AM (2000) Cap-Poly(A) synergy in mammalian cell-free extracts. Investigation of the requirements for poly(A)-mediated stimulation of translation initiation. *J Biol Chem* 275:32268–32276.
4. Kahvejian A, Svitkin YV, Sukarieh R, M'Boutchou MN, Sonenberg N (2005) Mammalian poly(A)-binding protein is a eukaryotic translation initiation factor, which acts via multiple mechanisms. *Genes Dev* 19:104–113.
5. Yanagiya A, et al. (2009) Requirement of RNA binding of mammalian eukaryotic translation initiation factor 4GI (eIF4GI) for efficient interaction of eIF4E with the mRNA cap. *Mol Cell Biol* 29:1661–1669.
6. Walsh D, Mathews MB, Mohr I (2013) Tinkering with translation: Protein synthesis in virus-infected cells. *Cold Spring Harb Perspect Biol* 5:a012351.
7. Ellison KS, Maranchuk RA, Mottet KL, Smiley JR (2005) Control of VP16 translation by the herpes simplex virus type 1 immediate-early protein ICP27. *J Virol* 79:4120–4131.
8. Fontaine-Rodriguez EC, Knipe DM (2008) Herpes simplex virus ICP27 increases translation of a subset of viral late mRNAs. *J Virol* 82:3538–3545.
9. Smith RWP, Graham SV, Gray NK (2008) Regulation of translation initiation by herpesviruses. *Biochem Soc Trans* 36:701–707.
10. Dobrikova E, Shveygert M, Walters R, Gromeier M (2010) Herpes simplex virus proteins ICP27 and UL47 associate with polyadenylate-binding protein and control its subcellular distribution. *J Virol* 84:270–279.
11. Salaun C, et al. (2010) Poly(A)-binding protein 1 partially relocalizes to the nucleus during herpes simplex virus type 1 infection in an ICP27-independent manner and does not inhibit virus replication. *J Virol* 84:8539–8548.
12. Gray NK, Hrabálková L, Scanlon JP, Smith RWP (2015) Poly(A)-binding proteins and mRNA localization: Who rules the roost? *Biochem Soc Trans* 43:1277–1284.
13. Spriggs KA, Bushell M, Willis AE (2010) Translational regulation of gene expression during conditions of cell stress. *Mol Cell* 40:228–237.
14. Larralde O, et al. (2006) Direct stimulation of translation by the multifunctional herpesvirus ICP27 protein. *J Virol* 80:1588–1591.
15. Fontaine-Rodriguez EC, Taylor TJ, Olesky M, Knipe DM (2004) Proteomics of herpes simplex virus infected cell protein 27: Association with translation initiation factors. *Virology* 330:487–492.
16. Gray NK, Coller JM, Dickson KS, Wickens M (2000) Multiple portions of poly(A)-binding protein stimulate translation in vivo. *EMBO J* 19:4723–4733.
17. Smith RWP, Malik P, Clements JB (2005) The herpes simplex virus ICP27 protein: A multifunctional post-transcriptional regulator of gene expression. *Biochem Soc Trans* 33:499–501.
18. Drummond DR, Armstrong J, Colman A (1985) The effect of capping and polyadenylation on the stability, movement and translation of synthetic messenger RNAs in Xenopus oocytes. *Nucleic Acids Res* 13:7375–7394.
19. Gorgoni B, Gray NK (2004) The roles of cytoplasmic poly(A)-binding proteins in regulating gene expression: A developmental perspective. *Brief Funct Genomics Proteomics* 3:125–141.
20. Smith RWP, Gray NK (2010) Poly(A)-binding protein (PABP): A common viral target. *Biochem J* 426:1–12.
21. Aubert M, Rice SA, Blaho JA (2001) Accumulation of herpes simplex virus type 1 early and leaky-late proteins correlates with apoptosis prevention in infected human HEp-2 cells. *J Virol* 75:1013–1030.
22. Michlewski G, Sanford JR, Cáceres JF (2008) The splicing factor SF2/ASF regulates translation initiation by enhancing phosphorylation of 4E-BP1. *Mol Cell* 30:179–189.
23. von Moeller H, et al. (2013) Structural and biochemical studies of SLIP1-SLBP identify DBP5 and eIF3g as SLIP1-binding proteins. *Nucleic Acids Res* 41:7960–7971.
24. Gorgoni B, et al. (2005) The stem-loop binding protein stimulates histone translation at an early step in the initiation pathway. *RNA* 11:1030–1042.
25. Jackson RJ (2005) Alternative mechanisms of initiating translation of mammalian mRNAs. *Biochem Soc Trans* 33:1231–1241.
26. Redondo N, et al. (2012) Translation directed by hepatitis A virus IRES in the absence of active eIF4F complex and eIF2. *PLoS One* 7:e52065.
27. Sweeney TR, Abaeva IS, Pestova TV, Hellen CU (2014) The mechanism of translation initiation on Type 1 picornavirus IRESs. *EMBO J* 33:76–92.
28. Pestova TV, Shatsky IN, Fletcher SP, Jackson RJ, Hellen CU (1998) A prokaryotic-like mode of cytoplasmic eukaryotic ribosome binding to the initiation codon during internal translation initiation of hepatitis C and classical swine fever virus RNAs. *Genes Dev* 12:67–83.
29. Hashem Y, et al. (2013) Hepatitis-C-virus-like internal ribosome entry sites displace eIF3 to gain access to the 40S subunit. *Nature* 503:539–543.
30. Ostareck DH, Ostareck-Lederer A, Shatsky IN, Hentze MW (2001) Lipoxygenase mRNA silencing in erythroid differentiation: The 3′UTR regulatory complex controls 60S ribosomal subunit joining. *Cell* 104:281–290.
31. Collier B, Gorgoni B, Loveridge C, Cooke HJ, Gray NK (2005) The DAZL family proteins are PABP-binding proteins that regulate translation in germ cells. *EMBO J* 24:2656–2666.
32. Svitkin YV, et al. (2001) Poly(A)-binding protein interaction with eIF4G stimulates picornavirus IRES-dependent translation. *RNA* 7:1743–1752.
33. Vende P, Piron M, Castagné N, Poncet D (2000) Efficient translation of rotavirus mRNA requires simultaneous interaction of NSP3 with the eukaryotic translation initiation factor eIF4G and the mRNA 3′ end. *J Virol* 74:7064–7071.
34. Burgess HM, Gray NK (2010) mRNA-specific regulation of translation by poly(A)-binding proteins. *Biochem Soc Trans* 38:1517–1522.
35. Smith RWP, et al. (2011) DAZAP1, an RNA-binding protein required for development and spermatogenesis, can regulate mRNA translation. *RNA* 17:1282–1295.
36. Mears WE, Rice SA (1996) The RGG box motif of the herpes simplex virus ICP27 protein mediates an RNA-binding activity and determines in vivo methylation. *J Virol* 70:7445–7453.
37. Sakoda Y, Ross-Smith N, Inoue T, Belsham GJ (2001) An attenuating mutation in the 2A protease of swine vesicular disease virus, a picornavirus, regulates cap- and internal ribosome entry site-dependent protein synthesis. *J Virol* 75:10643–10650.
38. Wadd S, et al. (1999) The multifunctional herpes simplex virus IE63 protein interacts with heterogeneous ribonucleoprotein K and with casein kinase 2. *J Biol Chem* 274:28991–28998.
39. Burgui I, Aragón T, Ortín J, Nieto A (2003) PABP1 and eIF4GI associate with influenza virus NS1 protein in viral mRNA translation initiation complexes. *J Gen Virol* 84:3263–3274.
40. Khaleghpour K, et al. (2001) Dual interactions of the translational repressor Paip2 with poly(A) binding protein. *Mol Cell Biol* 21:5200–5213.
41. Muddashetty R, et al. (2002) Poly(A)-binding protein is associated with neuronal BC1 and BC200 ribonucleoprotein particles. *J Mol Biol* 321:433–445.

Supporting Information

Smith et al. 10.1073/pnas.1610417114

SI Materials and Methods

Plasmids.

Tether-function MS2-fusion plasmids. MS2-fusion plasmids pMSPN (expressing MS2 coat protein), pMS2-U1A, pMS2-PAB (PABP1), pMS2 1-2 (PABP1 RRM1-2) (16), and pMS2-mDazl (31), as well as the construct encoding the MS2-xSLBP fusion protein (24), were described previously. pMSPN27 (expressing MS2-ICP27) was constructed as follows. The ICP27 ORF was amplified using PCR primers 5′-AAACT CGAGA TGGCG ACTGA CATTG ATATG CTAAT TG and 5′-CCTCG GATCC CTAAA ACAGG GAGTT GCAAT AAAAA TATTT GCC. The PCR product was inserted into the XhoI/BamHI sites of pMSPN. pMSPN-M15 and pMSPN-M16 were created by PCR amplification of the 3′ 302 bp of the mutant M15 and M16 ORFs from viral DNA using primers 5′-ATATA CACAG TGTGT TCGCG GCGGC GTC and 5′-CCTCG GATCC CTAAA ACAGG GAGTT GCAAT AAAAA TATTT GCC. The NsiI-BamHI fragment of pMSPN27 was exchanged with the corresponding PCR products. pMSPN-*d*0-4 (expressing MS2 fused to ICP27 amino acids 139–512) was made by exchanging a DraIII-NsiI fragment containing the *d*3-4 deletion (amino acids 109–138) from pM*d*3-4 (ref. 21 and references therein) with the corresponding fragment in pMSPN27, cutting with XhoI (removing the sequence encoding amino acids 1–138), and religating. pMSPN-*d*0-6 (expressing MS2 fused to ICP27 amino acids 175–512) was made by exchanging a DraIII-NsiI fragment containing the *d*5-6 deletion (amino acids 153–174) from pCITE-*d*5-6 (36) with the corresponding fragment in pMSPN27, cutting with XhoI (removing the sequence encoding amino acids 1–174), and religating. pMSPN-*d*0-7 (expressing MS2 fused to ICP27 amino acids 201–512) was made by exchanging a DraIII-NsiI fragment containing the *d*6-7 deletion (amino acids 174–200) from pM27-*d*6-7, a pM27 (ref. 21 and references therein) mutant containing this deletion, with the corresponding fragment in pMSPN27, cutting with XhoI (removing the sequence encoding amino acids 1–200), and religating. pM*d*3-4, pCITE-*d*5-6, and pM27-*d*6-7 were kindly provided by Stephen Rice (University of Minnesota, Minneapolis, MN).

Tether-function reporter constructs. pLG-MS2 (expressing Luc-$MS2_3$), pLGENB1 (expressing Luc-ΔMS2) (16), pLuc-MS2-pA (expressing Luc-$MS2_3$-pA), pJK350 (expressing the β-gal internal control mRNA) (31), PV-IRES-Luciferase-$MS2_3$, and CSFV-IRES-Luciferase-$MS2_3$ reporter constructs (24) were previously described. pHAV-Luc (expressing HAV-IRES-Luc-$MS2_3$) was constructed as follows. The sequence encoding the HAV IRES and N-terminal 48 amino acids of the HAV capsid protein (GenBank accession no. M14707.1; nucleotides 48–884) was amplified using primers 5′-TTTTA AGCTT GGTGA GGGGA CTTGA TACC and 5′-CCCCA AGCTT TGATC CACAG AAGTA AAATA AG. The resulting fragment was inserted in-frame with the luciferase gene into the unique HindIII site of pLG-MS2. pCSFV-*lacZ* expressing the CSFV-IRES-*lacZ* internal control was constructed as follows. The sequence containing the CSFV IRES and encoding the N-terminal 23 amino acids of the CSFV polyprotein was amplified from pCSFV-CAT (24) with primers 5′-CAGTC AGGAT CCGTC GACAA GGTTA GCTC and 5′-CAGTC AGGAT CCGGT TCCTC CACTC CCACT GGT. The PCR product was inserted in-frame with the *lacZ* gene into the unique BamHI site of pJK350. pCSFV-CAT was kindly provided by Matthias Hentze (European Molecular Biology Laboratory, Heidelberg, Germany).

Plasmids used for the 2A protease assay. pGEM-hU1A was previously described (16). Swine vesicular disease virus 2A protease was expressed from pGEM3Z/J1 (37), a gift from Graham Belsham (Technical University of Denmark, Kongens Lyngby, Denmark).

VP16 expression plasmid. The sequence corresponding to the complete VP16 mRNA, including the 5′ UTR and 3′ UTR, was amplified with primers 5′-TTTTC TAGAG TCATT CCTCG GGAAC GGACG and 5′-TTTGC TCAGC GGTTT TGTAA TGTAT GTGCT CGTG from DNA purified from BHK cells infected with HSV-1 strain 17 (National Center for Biotechnology Information accession no. NC_001806.2) using DNAzol (Invitrogen). The resulting product was inserted into the XbaI and BlpI sites of pET52b(+) (Novagen), yielding pET-VP16.

Y2H plasmids. Fusions of ICP27 truncations to the GAL4 DNA-binding domain (DNA-BD) [p502CBD (amino acids 10–512), p270CBD (amino acids 242–512), and pN397BD (amino acids 10–379)] were previously described (38). The same truncations were fused to the GAL4-activation domain using the unique BamHI and EcoRI sites of pACT2 (Clontech) to create p502CAD, p270CAD, and pN397AD. Fusions of M15 and M16 mutants (amino acids 10–512) to the GAL4 DNA-BD and DNA activation domains were made by exchanging DraIII-BsiWI ICP27 fragments containing the M15 or M16 mutations from pMSPN-M15 and pMSPN-M16, respectively, with the corresponding wild-type fragments in 502CBD (creating pM15-CBD and pM16-CBD) and 502CAD (creating pM15-CAD and pM16-CAD). PABP1 truncation plasmids used in the Y2H assay (PAB1-2, PAB3-4, PAB-Ct, PAB1-2Nt, and PAB-Rd), pACT-IRP, pACT-4GNt, pACT-Paip1, and LexA-MS2 were previously described (16).

Protein expression plasmids. GST-ICP27 was expressed from pGEX-27 (36), kindly supplied by Stephen Rice (University of Minnesota, Minneapolis, MN). pGST-1–261 was made by inserting a 0.8-kb BamHI-SalI fragment from pGEX-27 (encoding ICP27 amino acids 1–261) into the BamHI and SalI sites of pGEX-5X-3 (Amersham Bioscience) in-frame with the GST coding sequence. pGST-12–397 was made by inserting a 1.2-kb EcoRI-BamHI fragment from pN397BD (encoding ICP27 amino acids 12–397) into the EcoRI and NotI sites of pGEX-5X-1 (Amersham Bioscience) using a BamHI-NotI adaptor. pGST-12–512 was made by inserting a 1.5-kb EcoRI-BamHI fragment from p502CBD (encoding ICP27 amino acids 12–512) (38) into the EcoRI and NotI sites of pGEX-5X-1 (Amersham Bioscience) using a BamHI-NotI adaptor. pGST27-72–512 was made by inserting a 1.3-kb EcoRI-BamHI fragment from p440CBD (encoding ICP27 amino acids 72–512) (38) into the EcoRI and NotI sites of pGEX-5X-1 using a BamHI-NotI adaptor. His-ICP27 was expressed from pET63, which contains the ICP27 ORF cloned into the SacI and BamHI sites downstream of the T7 promoter in pET28c (Novagen). His-PABP1 was expressed from pET-hPABP1 (35). GST-PABP1 was expressed from pGEX-2T-PABP1 (39), kindly provided by Amelia Nieto (Consejo Superior de Investigaciones Cientificas, Madrid, Spain). Plasmids expressing GST fusions of PABP1 domains were described previously [pGEX6P-PABP1-RRM1-HA, pGEX6P-PABP1-RRM2-HA, pGEX6P-PABP1-RRM3-HA, pGEX6P-PABP1-RRM4-HA, pGEX6P-PABP1-RRM1+2-HA, pGEX6P-PABP1-RRM2+3-HA, pGEX6P-PABP1-RRM3+4-HA, pGEX6P-PABP1-C1-HA, and pGEX6P-PABP1-C2-HA (40)], which were kind gifts from Nahum Sonenberg, (McGill University, Montreal, QC, Canada), as well as pPABP1-C5 (41), kindly provided by Jürgen Brosius (University of Münster, Muenster, Germany). The pGST–PABP1–C-terminal domain contains a fragment of human PABP1 cDNA encoding the C-terminal region (amino acids 388–636). This region was PCR-amplified with primers 5′-GAGCG GATCC CAAGT GTACG AGCTG TTC and 5′-GCGCG AATTC TTAAA CAGTT GGAAC ACCGG. The product was inserted into the BamHI and EcoRI sites of pGEX-5X-3.

Cells and Viruses. BHK C13 cells, wild-type HSV-1, ICP27-mutant strains carrying the M15 and M16 point mutations, and the ICP27-deficient mutant 27lacZ were grown as described elsewhere (21, 38).

Antibodies. Primary antibodies were as follows: ICP27 1113 and 1119 (Virusys; diluted 10^{-4}), PABP1 monoclonal 10E10 (Abcam; diluted 10^{-4}), PABP1 polyclonals (Covalab; diluted 2×10^{-4}), GAPDH (no. H86504M, AMS Biotechnology; diluted 10^{-3}), GST (no. 27-4577-01, Amersham; diluted 10^{-4}), polyhistidine (Sigma; diluted 10^{-3}), eIF4G and Paip1 (kindly provided by S. Morley, University of Sussex, Brighton, UK; diluted 10^{-4} and 2×10^{-4}, respectively), VP16 ab4808 (Abcam; diluted 3×10^{-4}), and ePABP (diluted 10^{-3}) (31). Secondary antibodies were horseradish peroxidase-conjugated anti-rabbit (Sigma; diluted 10^{-5}), anti-mouse (Pierce; diluted 10^{-4}), or anti-goat (Sigma; diluted 10^{-3}) IgG for detection by enhanced chemiluminescence (GE Healthcare) and Alexa Fluor 680 goat anti-rabbit or anti-mouse (Invitrogen; diluted 10^{-4}) for quantitative analysis using an Odyssey Infrared Imager (LI-COR Biosciences).

Translational Stimulation of VP16 mRNA. *Xenopus laevis* oocytes were injected with 50 ng of mRNAs (transcribed in vitro from pET63 and pGEM-hU1A) expressing ICP27 or U1A (negative control). After allowing protein expression, the oocytes were injected with VP16 mRNA (50, 250, or 500 pg; transcribed in vitro from pET-VP16), along with a luciferase reporter mRNA (Fig. S2*A*, [1]) as an internal control to adjust for differences in mRNA injection efficiency, and incubated overnight. VP16 protein was assayed by quantitative immunoblotting and normalized to luciferase activity levels.

Modified Tether-Function Assay with 2A Protease. In these assays, the reporter mRNA mix (50 nL per oocyte) contained 20 ng/μL m^7GpppG-Luc-MS2 mRNA and 70 ng/μL ApppG-capped, unadenylated CSFV-*lacZ* mRNA alongside 0.4 μg/μL m^7GpppG-capped U1A mRNA or 2A protease mRNA. Oocytes were incubated for a further 3 h before assay. Data are from a minimum of three independent experiments, with the translation level of MS2 alone set to 1. Error bars indicate SEM. Statistical analysis was performed with a two-tailed unpaired Student's *t* test. $P \leq 0.05$ was considered significant.

RNA Stability Analysis. Total RNA was extracted from injected oocytes (same method as used for tether-function assay) using Tri Reagent (Sigma), and first-strand cDNA was synthesized from total RNA with an AMV Reverse Transcriptase Kit (Roche) according to the manufacturer's instructions. Quantitative RT-PCR analysis was performed with an ABI 7500 Fast Real-Time PCR System (ABI) by SYBR I green incorporation with luciferase primers 5′-GGCGC GGTCG GTAAA GTT and 5′-AGCGT TTTCC CGGTA TCCA. Data analysis was performed with AB17500 software. Mean threshold cycle (Ct) values were plotted with error bars representing SEM.

Gel Electrophoresis and Immunoblotting. Denatured protein samples were resolved on 10% SDS/PAGE or 4–12% Bis-Tris gradient gels (Invitrogen) and transferred to Immobilon-P or Immobilon-FL membranes (Millipore) for detection by enhanced chemiluminescence (GE Healthcare) or for quantitative analysis using an Odyssey Infrared Imager, respectively.

Protein Expression and Purification. GST-ICP27 and truncations were expressed in 200-mL cultures of *Escherichia coli* BL21 (DE3) pLysS (Novagen) after a 4-h induction with 1 mM isopropyl-β-D-thiogalactopyranoside (IPTG) at 25 °C. Bacteria were lysed in 10 mL of 50 mM Tris·HCl (pH 8), 100 mM NaCl, 1× BugBuster (Novagen), 1,000 U/mL lysozyme (Novagen), and 25 U/mL Benzonase (Novagen), containing protease inhibitor mixture (Roche). Cell debris was removed by centrifugation. Lysates were incubated with preswollen glutathione 4B Sepharose beads (Amersham Pharmacia) for 3 h at 4 °C with rotation before washing four times in 5 mL of 50 mM Tris·HCl (pH 8), 150 mM NaCl, and 0.1% Nonidet P-40. Bound protein was eluted in 50 mM Tris·HCl (pH 8), 150 mM NaCl, 1.5 mM $MgCl_2$, 0.5 mM DTT, 20 mM reduced glutathione, and 20% glycerol, and stored at −80 °C.

GST-PABP1 and truncations were expressed during a 3.5-h induction with 1 mM IPTG at 30 °C. Bacteria were lysed in PBS (pH 7.4) containing 1× BugBuster, 1 mM DTT, 5 mg/mL lysozyme, 50 U/mL Benzonase, 500 U/mL RNase 1 (Ambion), and protease inhibitor mixture (Roche). Cell debris was removed by centrifugation, and lysates were incubated with preswollen glutathione 4B Sepharose beads for 3 h at 4 °C with rotation before washing five times in 5 mL of PBS and eluting in 50 mM Tris·HCl (pH 8), 20 mM reduced glutathione, and 33% glycerol. Aliquots were stored at −80 °C. Purified FLAG-eIF4G was a gift from Simon Morley, University of Sussex, Brighton, UK.

His-ICP27 was expressed in a 500-mL culture during a 4-h induction with 1 mM IPTG at 25 °C. Bacteria were lysed in 10 mL of 50 mM Tris·HCl (pH 8), 100 mM NaCl, 0.5 mM DTT, 0.05% Nonidet P-40, 1× BugBuster, 1,000 U/mL lysozyme, and 25 U/mL Benzonase containing EDTA-free protease inhibitor mixture (Roche). Cell debris was removed by centrifugation, and lysates were incubated with 0.5 mL of nickel-nitrilotriacetic acid (Ni-NTA) agarose (Qiagen) for 1 h at 4 °C with rotation. Beads were washed six times in 10 mL of 50 mM Tris·HCl (pH 8), 200 mM NaCl, 20 mM imidazole, 0.5 mM DTT, and 0.05% Nonidet P-40. Protein was eluted in 0.5-mL fractions in 50 mM Tris·HCl (pH 8), 150 mM NaCl, 1.5 mM $MgCl_2$, 0.5 mM DTT, 250 mM imidazole, and 20% glycerol, and stored at −80 °C.

His-PABP1 was expressed in a 200-mL culture during a 3.5-h induction with 1 mM IPTG at 22 °C. Bacteria were lysed in 5 mL of PABP lysis buffer [20 mM Tris·HCl (pH 8), 150 mM NaCl, 10 mM imidazole, 1 mM DTT, 1× BugBuster, 1,000 U/mL lysozyme, 25 U/mL Benzonase] containing EDTA-free protease inhibitor mixture (Roche). Cell debris was removed by centrifugation, and lysates were incubated with 0.5 mL of Ni-NTA agarose for 2 h at 4 °C with rotation. Beads were washed once in PABP lysis buffer and twice in 20 mM Tris·HCl (pH 8), 300 mM NaCl, 10 mM imidazole, and 1 mM DTT. Protein was eluted in 0.5-mL fractions in 20 mM Tris·HCl (pH 8), 150 mM NaCl, 250 mM imidazole, and 1 mM DTT. Proteins were resolved by SDS/PAGE and visualized with Gelcode Blue (Pierce).

GST Pull-Down Assay. Before pull-downs, purified proteins were visualized by SDS/PAGE and SYPRO Ruby (Invitrogen) staining and full-length proteins were quantified using a phosphoimager with a BSA dilution series as standards. Three picomoles of GST/GST-PABP1 or His-PABP1 and 15 pmol of His-ICP27 or GST/GST-ICP27/GST-ICP27 truncations were incubated with 50 μL of equilibrated glutathione Sepharose in 1.5 mL of binding buffer [50 mM Tris·HCl (pH 8), 100 mM NaCl, 0.1% Nonidet P-40, 500 U/mL RNase 1] for 3 h at 4 °C and washed six times in 50 mM Tris·HCl (pH 8), 200 mM NaCl, and 0.1% Nonidet P-40. For the ternary complex, 15 pmol of GST/GST-ICP27, 15 pmol of His-PABP1, and 10 pmol of FLAG-tagged eIF4G were incubated with 30 μL of glutathione Sepharose for 3 h at 4 °C in 1.3 mL of 50 mM Tris·HCl (pH 8), 100 mM NaCl, 1.5 mM $MgCl_2$, and 0.05% Nonidet P-40 before washing three times in the same buffer. For pull-downs with cell extracts, 5 μg of GST-PABP1 (or truncations) was incubated for 3 h at 4 °C with 100 μg of HSV-1–infected BHK cell extract and 50 μL of glutathione Sepharose in 1 mL of binding buffer. Beads were washed five times in 50 mM Tris·HCl (pH 8), 150 mM NaCl, and 0.1%

Nonidet P-40. Protein was eluted in 20 μL of loading buffer for 5 min at 90 °C and analyzed by immunoblotting.

Y2H Analysis. Y2H analyses were performed with the MaV99 and L40*ura*$^-$ yeast strains as described elsewhere (24). ICP27 lacks the first nine amino acids, which cause *trans*-activation by ICP27 alone (38).

Coimmunoprecipitations. One hundred micrograms of cell extract was mixed with 100 ng of anti-ICP27 antibodies 1113 and 1119 (Virusys), 100 ng of mouse IgG (Sigma), or normal mouse serum in 500 μL of buffer E [100 mM Tris·HCl (pH 7.4), 100 mM NaC1, 1% Nonidet P-40, 0.5% Na deoxycholate] containing protease inhibitor mixture (Roche) for 2 h at 4 °C with or without 5 μg of RNase A (Ambion), 100 units of RNase 1 (Sigma), or 200 units of RNase T1 (Sigma) per 100 μg of total protein. One hundred fifty microliters of protein A-Sepharose was added and incubated for 3 h at 4 °C. Resin was washed six times with buffer E and eluted in 50 μL of loading buffer [50 mM Tris·HCl (pH 6.8), 100 mM DTT, 2% SDS, 0.1% bromophenol blue, 10% glycerol]. Samples were analyzed by immunoblotting.

RNA coimmunoprecipitation was carried out from oocytes microinjected with 50 ng of MS2 or MS2-ICP27 mRNA, incubated for 6 h, microinjected with 25 pg of ApG-capped luciferase reporter mRNA, and incubated for 3 h. Oocytes were mechanically lysed in 10 μL per oocyte of 20 mM Hepes (pH 7.6), 10 mM KCl, 1.5 mM $MgCl_2$, 100 mM NaCl, 5 mM NaF, 1 mM DTT, 800 U/mL RNasin (Promega), 0.5% Triton X-100, and 0.5% Na deoxycholate containing protease inhibitor mixture. ePABP [the major PABP family member expressed in oocytes (31)] was immunoprecipitated with 0.5 μg of anti-ePABP antibody per milligram of total protein or rabbit IgG as a control in the presence of 50 μL of protein A-Sepharose for 2 h at 4 °C. Beads were washed seven times in 20 mM Hepes (pH 7.6), 10 mM KCl, 1 mM $MgCl_2$, 350 mM NaCl, and 0.05% Nonidet P-40. Samples were evenly split for protein and RNA analysis. Protein was analyzed as above. RNA was purified using Tri Reagent (Sigma) and analyzed by 25-cycle amplification using Titan One Tube RT-PCR (Roche) with primers 5′-GGCGC GGTCG GTAAA GTT and 5′-AGCGT TTTCC CGGTA TCCA (luciferase) or 5′-TGGTG ACAAT GCCAT GTTC and 5′-GATAA TGGAT CTGGT ATGTG (β-actin).

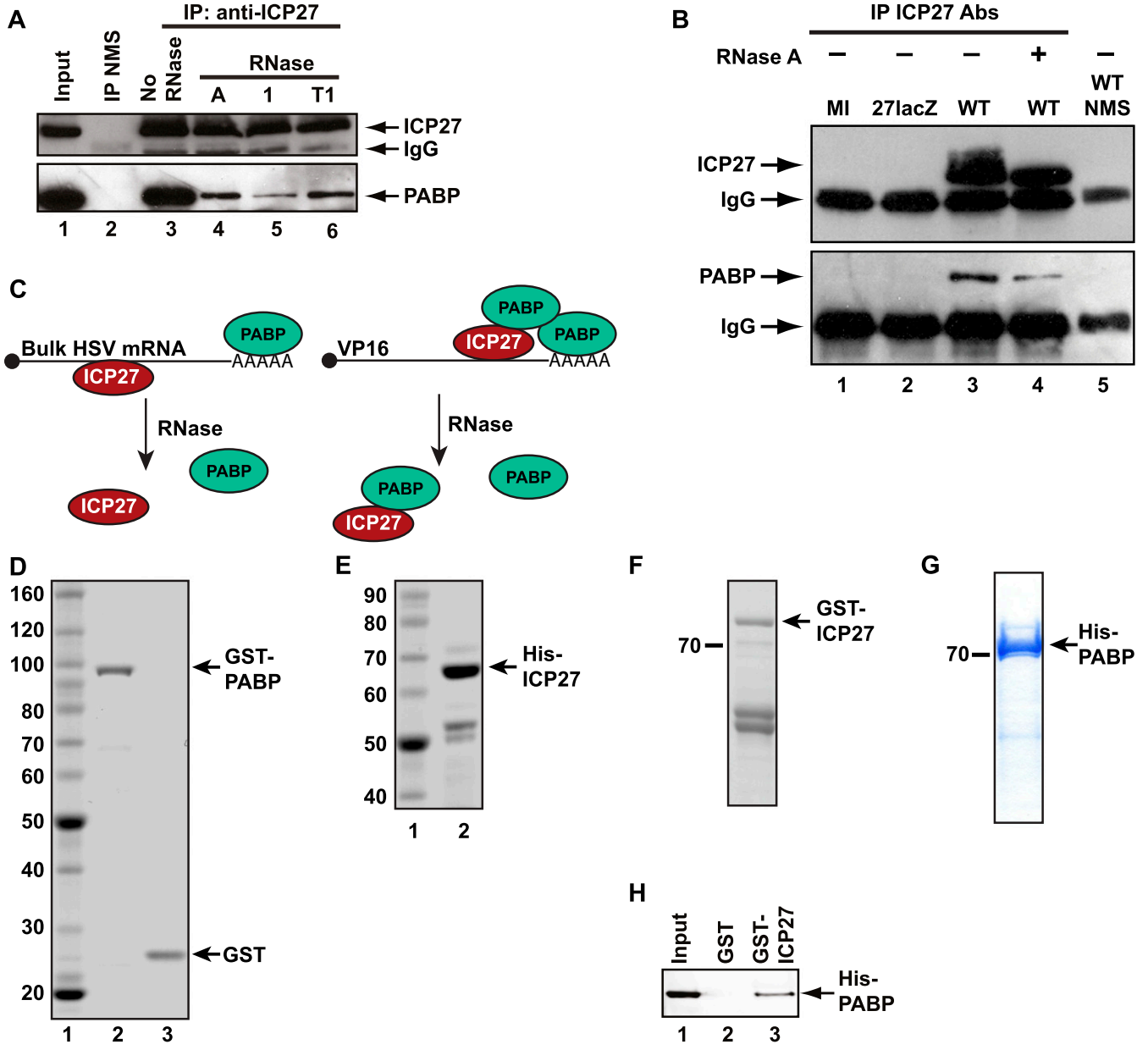

Fig. S1. ICP27 associates with PABP in vivo, and PABP interacts directly with ICP27 in vitro. (*A* and *B*) PABP specifically coimmunoprecipitates with ICP27 from HSV-1–infected BHK cell extracts, prepared 5 h postinfection. (*A*) HSV-1 (KOS 1.1)–infected cell extracts were incubated with normal mouse serum (NMS) (lane 2) or anti-ICP27 monoclonal antibodies 1113 and 1119 (lanes 3–6) in the absence (lane 3) or presence of RNase A, 1, or T1 (lanes 4–6). IP, immunoprecipitation. ICP27 (*Upper*) or PABP (*Lower*) was detected by immunoblotting. (*Upper*) Lower band in the upper panel is IgG heavy chain. (*B*) Wild type (WT; KOS 1.1) HSV-1, ICP27-null (27*lacZ*) HSV-1 (where the gene encoding ICP27 is replaced by *lacZ*), or mock-infected (MI) BHK cell extracts were incubated with a mixture of anti-ICP27 monoclonal antibodies 1113 and 1119 (lanes 1–4) or NMS (lane 5). ICP27 (*Upper*) and coimmunoprecipitated PABP (*Lower*) were detected by immunoblotting. RNase A treatment is indicated by a + symbol. The lower protein band in each panel is the IgG heavy chain. PABP is only coimmunoprecipitated from infected cells expressing ICP27. (*C*) ICP27 and PABP interact directly on a subset of HSV-1 transcripts. The multifunctional ICP27 protein (red) binds to most viral mRNAs, which are polyadenylated and may therefore also bind PABP (green). This property allows for their fortuitous mRNA-mediated coisolation, which is RNase-sensitive. However, our data suggest that ICP27 stimulates the translation of a subset of transcripts (e.g., VP16) by directly recruiting additional PABP to these mRNAs (Fig. 5*A*). Consequently, on these mRNAs, ICP27 and PABP are present in a functional complex (mediated by protein–protein interactions) that is RNase-insensitive. (*D*–*G*) Expression and purification of recombinant proteins. Recombinant proteins were expressed in and purified from *E. coli* BL21 (DE3) pLysS by affinity chromatography, resolved by SDS/PAGE, and visualized with Gelcode Blue. Molecular masses (kilodaltons) are indicated. (*D*) GST and GST-PABP. Full-length His-ICP27 (*E*) and GST-ICP27 (*F*) are indicated. The lower doublet in *E* and *F* was identified by immunoblotting as characteristic N-terminal ICP27 breakdown products. (*G*) His-PABP. (*H*) Immobilized purified GST-ICP27 or GST was incubated with purified His-PABP. Coisolated PABP was detected by immunoblotting; input represents 150%.

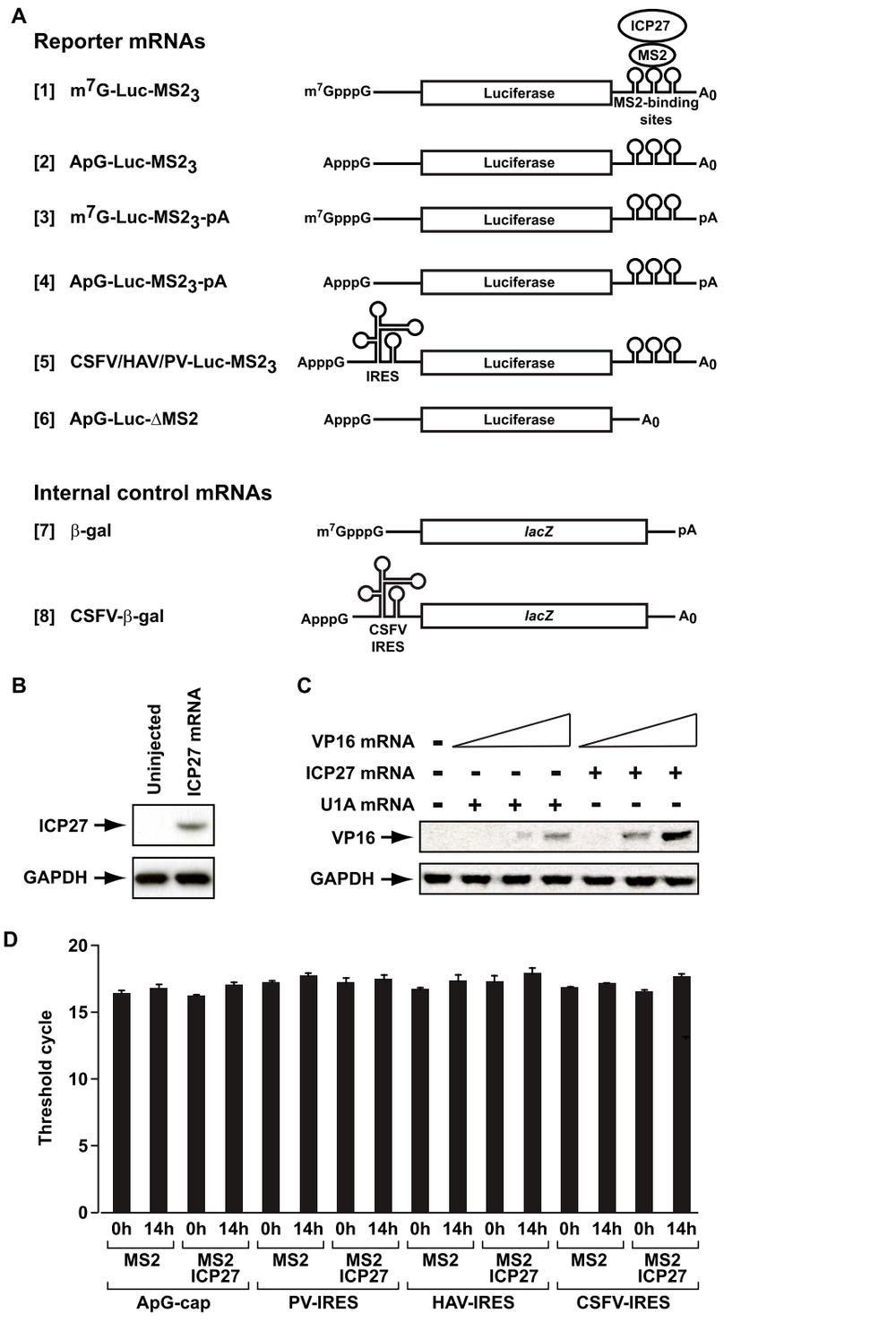

Fig. S2. Tether-function reporter mRNAs are stable in oocytes. (*A*) Diagram of reporter and internal control mRNAs used in the tether-function assays throughout this report. ICP27 is expressed in *X. laevis* stage VI oocytes as a fusion with the phage MS2 coat protein (MS2) and tethered to luciferase mRNA via the interaction of MS2 with three cognate-binding sites within the 3′ UTR (Luc-$MS2_3$). Reporter mRNAs are unadenylated, unless otherwise stated ([3], [4]), and have a 5′ m^7GpppG or ApppG cap (m^7G-Luc-$MS2_3$ [1], [3] and ApG-Luc-$MS2_3$ [2], [4]) or an IRES as indicated (CSFV-Luc-$MS2_3$, PV-Luc-$MS2_3$, or HAV-Luc-$MS2_3$ [5]) in the main text. IRES-reporter constructs are ApppG-capped. A luciferase reporter mRNA lacking the MS2-binding sites is designated ApG-Luc-ΔMS2 [6]. An m^7GpppG-capped polyadenylated *lacZ* mRNA containing no MS2-binding sites is used as an internal control (β-gal [7]). For the modified tether-function assay (Figs. 4*C* and 5*B*), an ApppG-capped, unadenylated, CSFV IRES-dependent internal control mRNA (CSFV–β-gal [8]) was used. (*B* and *C*) ICP27 alone is insufficient to activate VP16 mRNA translation efficiently. (*B*) *X. laevis* oocytes were injected with 50 ng of mRNA expressing ICP27, and ICP27 protein was detected by immunoblotting after overnight incubation. (*C*) In vitro-transcribed mRNA encoding VP16 (50, 250, or 500 pg) was injected into oocytes expressing either ICP27 or U1A (negative control), and VP16 protein was detected by immunoblotting after overnight incubation. (*D*) ICP27 does not affect reporter mRNA levels, consistent with the remarkable stability of mRNAs in oocytes (18). Oocytes expressing MS2 or MS2-ICP27 were injected with ApG-Luc-$MS2_3$, PV-Luc-$MS2_3$, HAV-Luc-$MS2_3$, or CSFV-Luc-$MS2_3$ reporter mRNAs. Total RNA was extracted either immediately (0h) or 14 h (14h) after injection and analyzed by quantitative RT-PCR with primers against the luciferase ORF, showing equivalent levels of mRNA. The number of amplification cycles required to obtain a detectable product in the linear range (threshold cycle) is shown. Error bars represent SEM.

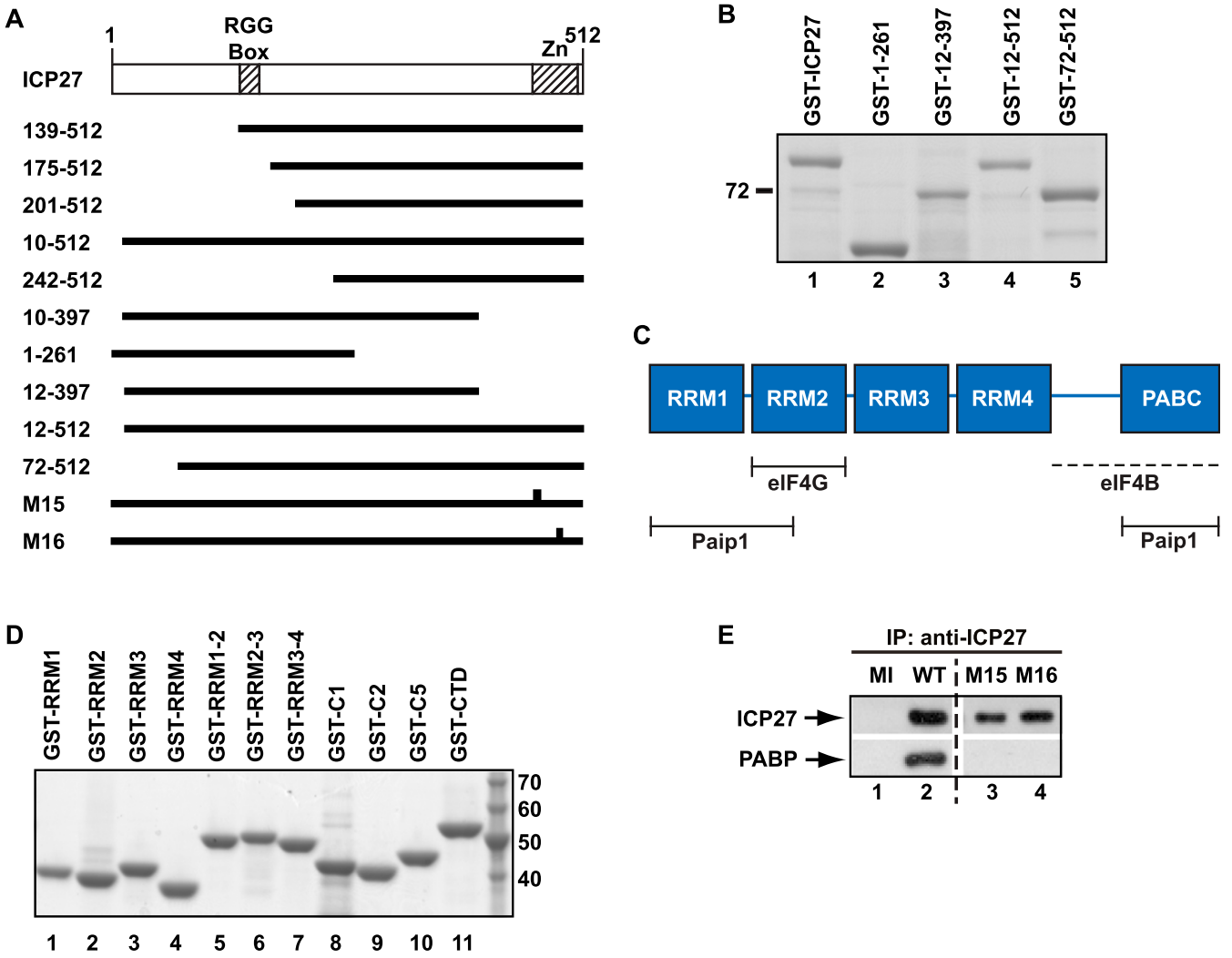

Fig. S3. ICP27 requires PABP binding to activate translation. (*A*) ICP27 deletion and point mutations used in this study. (*Upper*) Full-length ICP27 consists of 512 amino acids. RGG-box, RNA-binding domain; Zn, C-terminal zinc finger region. (*Lower*) Horizontal bars and gaps indicate amino acids present and absent, respectively. Vertical bars in M15 and M16 indicate the positions of point mutations. (*B*) Purification of GST fusions of ICP27 truncations. Recombinant proteins were expressed from the plasmids described in Table S2 and purified from *E. coli* BL21 (DE3) pLysS by affinity chromatography, resolved by SDS/PAGE, and visualized with Gelcode Blue. Molecular masses (kilodaltons) are indicated. (*C*) PABP contains four functionally nonequivalent RRM domains and a C-terminal region composed of a proline-rich linker (line) and the PABC domain. Minimal mapped binding regions for translation initiation factors are indicated (ref. 20 and references therein). Interaction with eIF4B requires integrity of the PABP C-terminal region (dotted line). (*D*) GST fusions of different PABP domains purified from the plasmids listed in Table S2 as described in Fig. S1. (*E*) PABP coimmunoprecipitates with WT, but not M15/M16 mutant ICP27 from HSV-1–infected cell extracts. HSV-1–infected cell extracts were incubated anti-ICP27 monoclonal antibodies 1113 and 1119. ICP27 expression (*Upper*) and coimmunoprecipitated PABP (*Lower*) were detected by immunoblotting. The dashed vertical line indicates removal of irrelevant lanes from the gel.

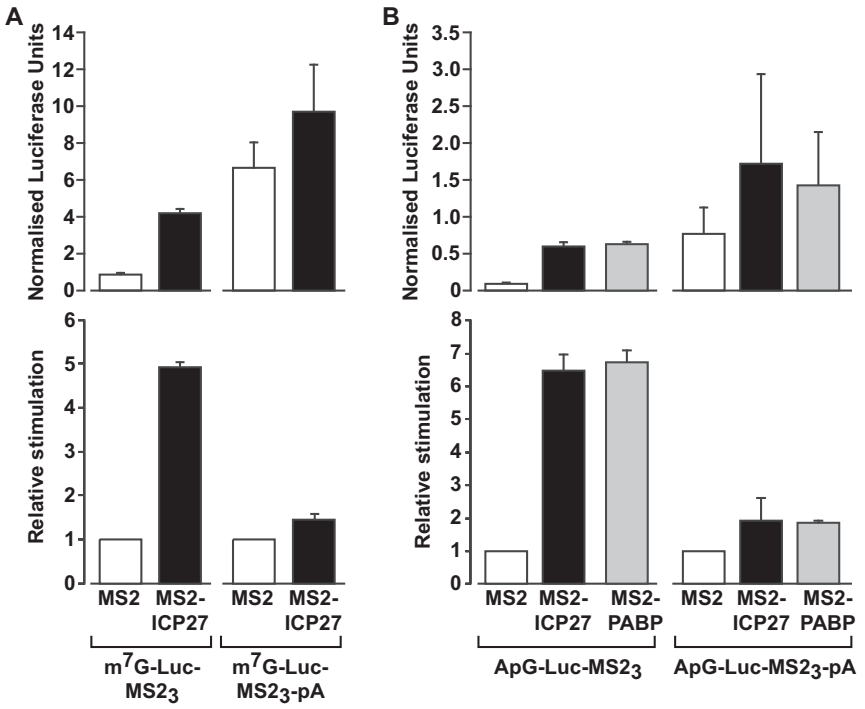

Fig. S4. ICP27-mediated translational activation is sensitive to reporter mRNA poly(A) tail length in a tether-function assay. (*A*) Oocytes expressing MS2 or MS2-ICP27 were coinjected with β-gal mRNA and m^7G-Luc-$MS2_3$ or an identical reporter mRNA with a 3′ poly(A) tail (m^7G-Luc-$MS2_3$-pA) (Fig. S2*A*, [7], [1], and [3], respectively). (*Upper*) Luciferase activity normalized to β-gal activity is plotted. (*Lower*) Relative stimulation compared with MS2 (set to 1) is plotted. (*Upper*) Polyadenylated reporter mRNA is translated more efficiently than its unadenylated counterpart, and translation of both reporters is stimulated by tethered ICP27. (*Lower*) Importantly, the relative increase in translational efficiency by ICP27 is greater with the unadenylated reporter than with the polyadenylated reporter. This result is consistent with ICP27 acting via recruitment of PABP, because this mode of action should result in a less pronounced stimulatory effect of MS2-ICP27 on polyadenylated reporter mRNAs, which will be bound by additional PABP molecules, compared with unadenylated reporter mRNAs, which can only recruit PABP via ICP27. (*B*) As in *A*, but substituting ApppG-capped for m^7GpppG-capped reporter mRNAs (ApG-Luc-$MS2_3$ and ApG-Luc-$MS2_3$-pA; Fig. S2*A*, [2] and [4], respectively) and with the inclusion of MS2-PABP. The use of ApppG-capped reporters [with or without a poly(A) tail], which are translated at a substantially reduced rate (Fig. S5*A*), excludes the possibility that the reduced relative stimulation by ICP27 observed in *A* is a consequence of a maximal translation level being reached. A similar result was observed when PABP was directly tethered. Taken together, these results provide strong support for a mechanism whereby ICP27 functions by facilitating the recruitment of PABP. Error bars denote SEM from three repeats.

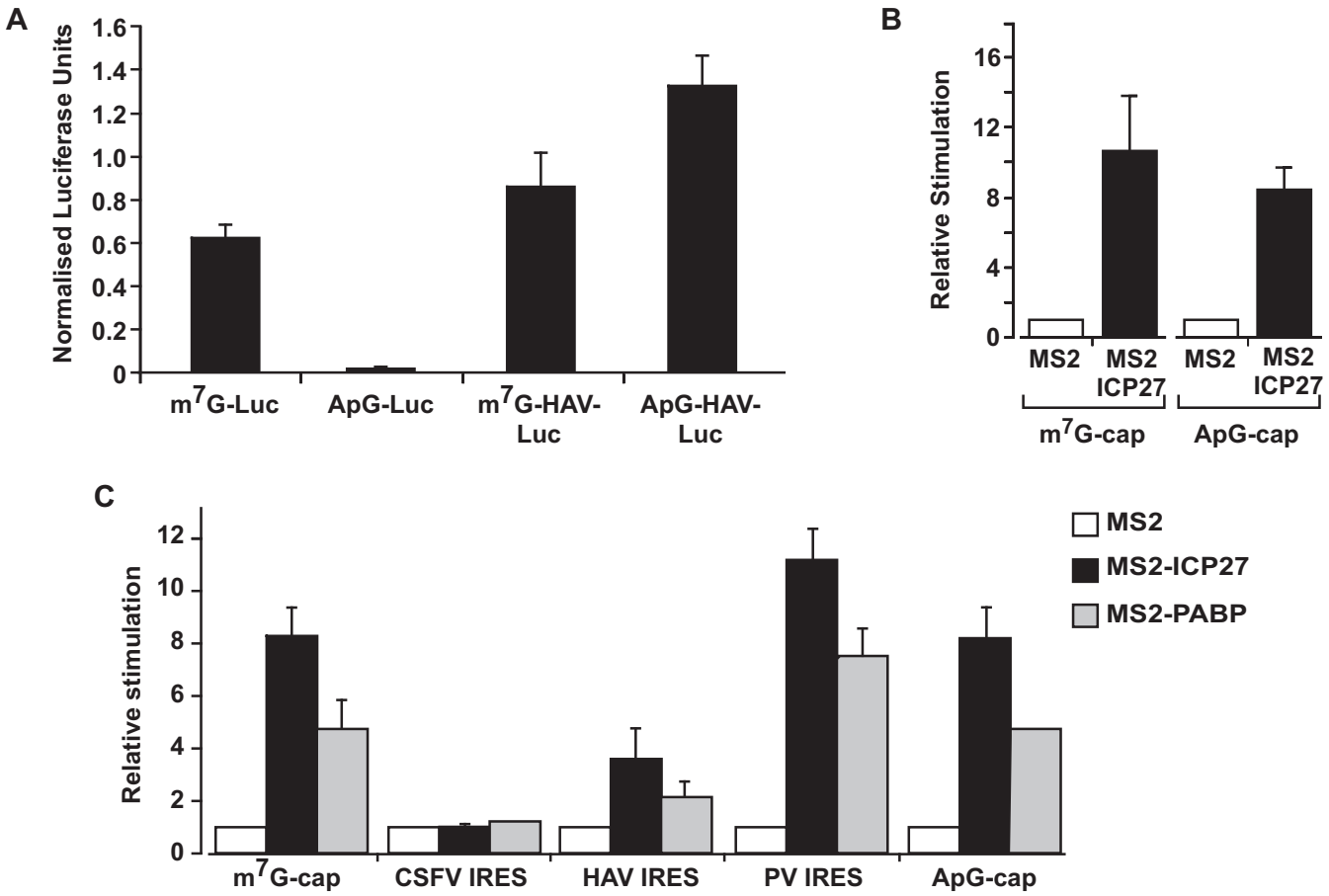

Fig. S5. (*A*) Translation in *X. laevis* oocytes is highly sensitive to the presence of a functional cap, and the HAV IRES is active in *X. laevis* oocytes. Oocytes were coinjected with 375 pg of β-gal internal control mRNA and 750 pg of of m^7G-Luc-MS2$_3$, ApG-Luc-MS2$_3$ (Fig. S2*A*, [1] and [2]), m^7GpppG-capped HAV-Luc-MS2$_3$, or ApppG-capped HAV-Luc-MS2$_3$ mRNAs. The former two mRNAs show that replacing the physiological m^7GpppG cap with ApppG results in a >70-fold reduction of translational efficiency. The latter two mRNAs contain the HAV IRES, although one is physiologically capped (m^7GpppG) and the other is not (ApppG). The presence of the HAV IRES promotes efficient translation of the ApppG-capped mRNA (compare ApG-HAV-Luc-MS2$_3$ versus ApG-Luc-MS2$_3$ and m^7G-Luc-MS2$_3$), showing that it is functional in oocytes. Luciferase activity normalized to β-gal activity is plotted. Error bars indicate SEM. (*B*) ICP27 activates a nonphysiologically (ApppG)-capped reporter mRNA in a tether-function assay. Oocytes expressing MS2 or MS2-ICP27 were coinjected with β-gal mRNA and m^7G-Luc-MS2$_3$ or ApG-Luc-MS2$_3$ (Fig. S2*A*, [1], [2] and [7]). Effects on translation were measured by luciferase assay normalized for β-gal activity. Translational stimulation relative to MS2 protein alone (set to 1) is plotted. Error bars indicate SEM from three repeats. (*C*) Translational activation of different reporter mRNAs by tethered full-length PABP recapitulates translational stimulation by tethered ICP27. Oocytes expressing MS2, MS2-ICP27, or MS2-PABP were coinjected with β-gal mRNA and m^7G-Luc-MS2$_3$ or CSFV-Luc-MS2$_3$ mRNA, HAV-Luc-MS2$_3$ mRNA, PV-Luc-MS2$_3$ mRNA, or ApG-Luc-MS2$_3$ mRNA (Fig. S2*A*, [7], [1], [5], and [2], respectively). Effects on translation were measured by luciferase assay normalized for minor changes in β-gal activity. Translational stimulation relative to translational stimulation of MS2 is plotted; error bars indicate SEM.

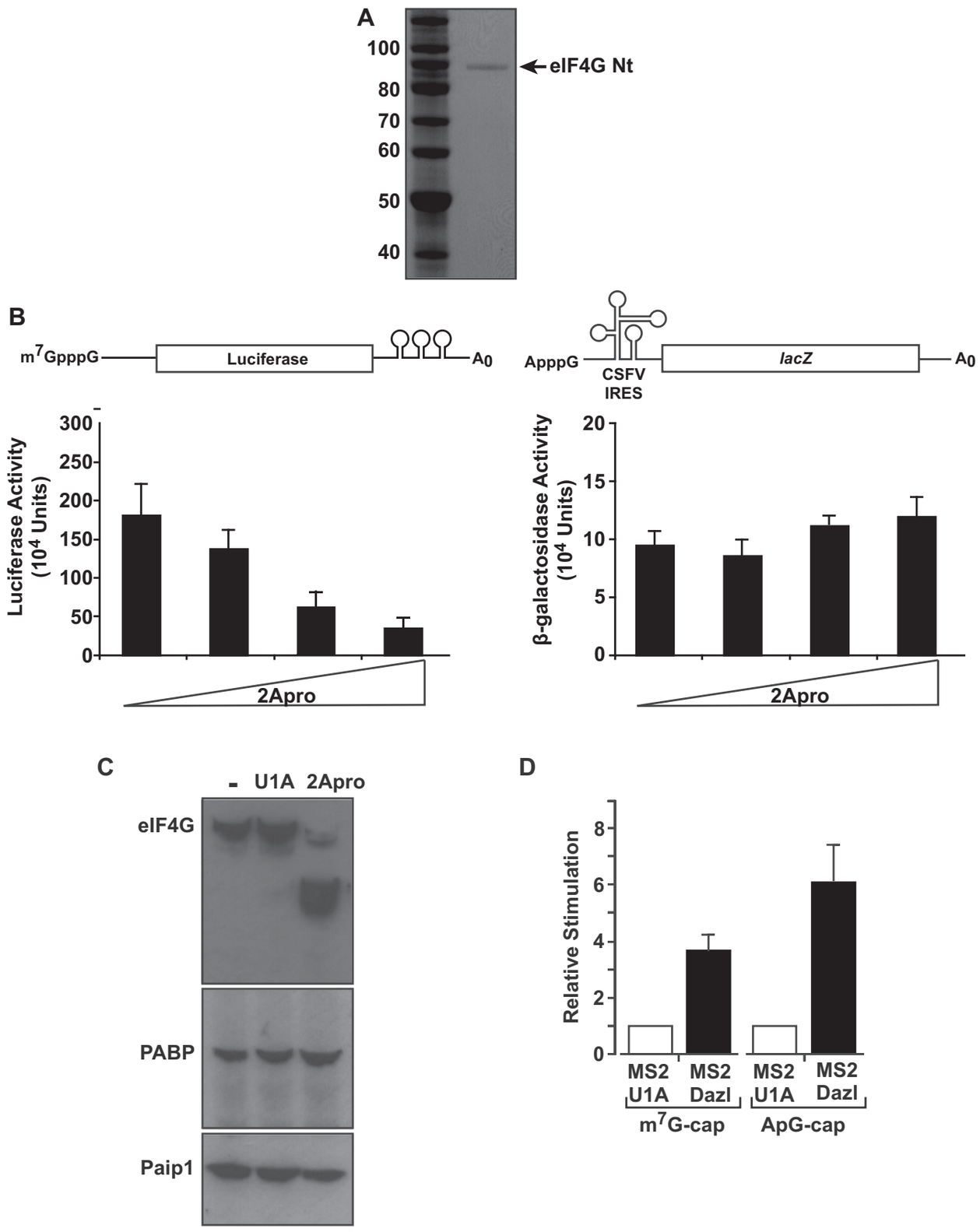

Fig. S6. (*A*) Purified eIF4G. FLAG fusion of eIF4G (amino acids 1–532) visualized with Gelcode Blue. (*B*) 2A protease does not disrupt CSFV IRES-dependent translation initiation. Oocytes were injected with m^7G-Luc-MS2$_3$ (*Left*) or CSFV–β-gal (*Right*) mRNAs (Fig. S2*A*, [3] and [8]) and increasing amounts of mRNA expressing 2Apro. Luciferase and β-gal activities were determined, showing that 2Apro inhibits cap-dependent (*Left*) but not eIF4G-independent (*Right*) CSFV IRES-driven translation, as expected. (*C*) Oocytes were uninjected (–) or injected with mRNA expressing 2Apro or U1A (a proteolytically and translationally inert control protein). After 3 h, extracts were prepared and endogenous eIF4G, PABP, and Paip1 were analyzed by immunoblotting. (*D*) Dazl activates a non-physiologically (ApppG)-capped reporter mRNA in a tether-function assay. Oocytes expressing MS2-U1A or MS2-Dazl were coinjected with β-gal mRNA and m^7G-Luc-MS2$_3$ or ApG-Luc-MS2$_3$ (Fig. S2*A*, [1], [2], and [7]). Effects on translation were measured by luciferase assay normalized for β-gal activity. Translational stimulation relative to MS2-U1A (set to 1) is plotted. Error bars indicate SEM from six repeats.

Table S1. Y2H analysis of the interaction of ICP27 and translation initiation factors

Binding domain	Activation domain	Interaction*
Lex A	ICP27	–
eIF4G Ct	ICP27	–
PABP Ct	ICP27	++++
ICP27	IRP	–
ICP27	PABP Ct	+++
ICP27	eIF1	–
ICP27	eIF1A	–
ICP27	eIF2α	+/–
ICP27	eIF2β	+/–
ICP27	eIF3 S1	–
ICP27	eIF3 S2	+/–
ICP27	eIF3 S3	–
ICP27	eIF3 S4	+
ICP27	eIF3 S5	+/–
ICP27	eIF3 S6	+/–
ICP27	eIF3 S7	+/–
ICP27	eIF3 S8	–
ICP27	eIF4A	+/–
ICP27	eIF4B	–
ICP27	eIF4E	+/–
ICP27	eIF4G Nt	–
ICP27	eIF4H	–
ICP27	eIF5	–
ICP27	eIF5A	–
ICP27	eIF5B	–
ICP27	Paip 1	–

Ct, C terminus; Nt, N terminus.

*Y2H interactions were determined with a β-gal filter assay as described (24). Color development is denoted by a + symbol, with multiple + symbols representing increasing intensity relative to the negative control. The symbol +/– represents faint color development in some colonies.

Table S2. GST-PABP1 and GST-ICP27 expression plasmids used in this study

Plasmid	GST fusion	Source
pGEX-2T-PABP1	GST-PABP1 full length	(39)
pGEX6P-PABP1-RRM1-HA	GST-PABP1 (amino acids 1–98)	(40)
pGEX6P-PABP1-RRM2-HA	GST-PABP1 (amino acids 99–190)	(40)
pGEX6P-PABP1-RRM3-HA	GST-PABP1 (amino acids 191–289)	(40)
pGEX6P-PABP1-RRM4-HA	GST-PABP1 (amino acids 290–368)	(40)
pGEX6P-PABP1-RRM1+2-HA	GST-PABP1 (amino acids 1–190)	(40)
pGEX6P-PABP1-RRM2+3-HA	GST-PABP1 (amino acids 98–289)	(40)
pGEX6P-PABP1-RRM3+4-HA	GST-PABP1 (amino acids 191–368)	(40)
pGEX6P-PABP1-C1-HA	GST-PABP1 (amino acids 369–494)	(40)
pGEX6P-PABP1-C2-HA	GST-PABP1 (amino acids 495–633)	(40)
pPABP1-C5	GST-PABP1 (amino acids 462–634)	(41)
pGST-PABP1-CTD	GST-PABP1 (amino acids 388-636)	This work
pGEX-27	GST-ICP27 full-length	(36)
pGST-1–261	GST-ICP27 (amino acids 1–261)	This work
pGST-12–397	GST-ICP27 (amino acids 12–397)	This work
pGST-12–512	GST-ICP27 (amino acids 12–512)	This work
pGST-72–512	GST-ICP27 (amino acids 72–512)	This work

CTD, C-terminal domain.